



AN ANALYSIS AND DESIGN OF A  
LINEAR GUARDED CUT-BAR APPARATUS  
FOR THERMAL CONDUCTIVITY MEASUREMENTS.

By

David A. Didion

Technical Report No. 2

Prepared Under Contract NONR 2249 (12)

for

Office of Naval Research  
Washington, D. C. 20390

31 January 1968

The Catholic University of America  
Department of Mechanical Engineering  
Washington, D. C. 20017



## ACKNOWLEDGEMENTS

It should be noted that the Analysis discussed in this report has been influenced by similar work in References [2] and [3]. Since these References are not readily available in the open literature Figure 11 and its related discussion have been included for the sake of completeness.

The author wishes to express his gratitude to Professor Michael Chi for his assistance with the mathematical analysis and Mr. L. Fisher for the programming and Figure construction.



## TABLE OF CONTENTS

|  | <u>Page</u> |
|--|-------------|
| Abstract . . . . .   | iv          |
| List of Figures . . . . .                                    | v           |
| Nomenclature . . . . .                                       | vi          |
| I. Introduction . . . . .                                    | 1           |
| II. Analysis . . . . .                                       | 5           |
| III. Design . . . . .  | 13          |
| IV. References . . . . .                                     | 25          |
| Appendices   |             |
| A. Mathematical Analysis of the Geometrical Factor . . . . . | 26          |
| B. Computer Program for the Geometrical Factor . . . . .     | 42          |

## ABSTRACT

A quantitative analysis of the Cut-Bar method of measuring the thermal conductivity of solids is performed. The mathematical model, which corrects for the difference in heat flux in the specimen and reference standard, is that of the two dimensional steady heat conduction equation applied to an annulus of insulation. The solution is presented in detail and found to be comprised of two physically distinct parts, a conductivity factor and a geometrical factor. A number of charts and graphs are presented for clarification as to the nature and magnitude the relative sizes of the various components will have on the accuracy over different conductivity ranges. The complexity of the geometrical factor required a digital computer programs which are included.

Reference is made to a similar study, performed by researchers at the National Bureau of Standards. It is found that the differences in the guard temperature distribution results in a substantial change in the geometrical factor.

## LIST OF FIGURES

| <u>Figures</u> |   | <u>Page</u> |
|----------------|---|-------------|
| 1.             | Cut-Bar Apparatus . . . . .   | 3           |
| 2.             | Temperatures on the Boundary Surfaces of the<br>Powder Insulation Annulus . . . . . | 4           |
| 3.             | Shunting of Heat Flux in a Cut-Bar Apparatus . . . . .                              | 8           |
| 4.             | Plot of the Geometrical Factor and Fractional Power<br>Change . . . . .             | 9           |
| 5.             | Computer Output . . . . .   | 10          |
| 6.             | Comparison of Geometrical Factors . . . . .   | 11          |
| 7.             | Geometrical Factor as a Function of the Ratio of<br>Apparatus Diameters . . . . .   | 12          |
| 8.             | Design Chart . . . . .  | 18          |
| 9.             | Design Chart for Optimum Dimensions . . . . .                                       | 19          |
| 10.            | Effect of Specimen Thermal Conductivity . . . . .                                   | 20          |
| 11.            | Maximum Errors for Various Ranges of Specimen<br>Thermal Conductivity . . . . .     | 21          |
| 12.            | Plot of the Fractional Power Change . . . . .                                       | 22          |
| 13.            | Computer Output . . . . .   | 23          |
| 14.            | Plot of the Geometrical Factor and Fractional Power<br>Change . . . . .             | 24          |
| A-1            | Schematic of the Cut-Bar Apparatus . . . . .  | 27          |
| B-1            | Computer Program Flow Chart . . . . .   | 45          |
| B-2            | Computer Program for IBM 1620 Computer . . . . .                                    | 46          |
| B-3            | Computer Program for Time Sharing Computer . . . . .                                | 53          |
| B-4            | Computer Program for Time Sharing Computer . . . . .                                | 60          |

## NOMENCLATURE

|        |   |   |
|--------|---|---|
| $A$    | - | RADIUS OF THE CUT-BAR, FT   |
| $A_m$  | - | CROSS SECTIONAL AREA OF THE METER-BAR, $\text{FT}^2$  |
| $A_s$  | - | CROSS SECTIONAL AREA OF SPECIMEN BAR, $\text{FT}^2$   |
| $a$    | - | NON-DIMENSIONAL RADIUS, $\frac{A}{W}$   |
| $a_n$  | - | EULER COEFFICIENTS, $n = 1, 2, 3, \dots$  |
| $B$    | - | OUTER RADIUS OF THE ANNULUS, FT   |
| $B_c$  | - | CRITICAL OUTER RADIUS OF THE ANNULUS, FT  |
| $b$    | - | NON-DIMENSIONAL OUTER RADIUS OF THE ANNULUS, $\frac{B}{W}$  |
| $b_n$  | - | EULER COEFFICIENTS, $n = 1, 2, 3, \dots$  |
| $C_n$  | - | CONSTANTS, $n = 1, 2, 3, \dots$   |
| $D_n$  | - | CONSTANTS, $n = 1, 2, 3, \dots$   |
| $F_g$  | - | GEOMETRICAL FACTOR, DIMENSIONLESS   |
| $F_k$  | - | THERMAL CONDUCTIVITY FACTOR, DIMENSIONLESS  |
| $G(Z)$ | - | TEMPERATURES ALONG THE INNER CYLINDRICAL SURFACE OF THE ANNULUS, $^{\circ}\text{F}$                                     |
| $g(u)$ | - | NON-DIMENSIONAL TEMPERATURES ALONG THE INNER CYLINDRICAL SURFACE OF THE ANNULUS   |
| $H(Z)$ | - | TEMPERATURES ALONG THE OUTER CYLINDRICAL SURFACE OF THE ANNULUS, $^{\circ}\text{F}$                                     |
| $h(u)$ | - | NON-DIMENSIONAL TEMPERATURES ALONG THE OUTER CYLINDRICAL SURFACE OF THE ANNULUS   |
| $I_v$  | - | MODIFIED BESSEL FUNCTION OF THE FIRST KIND OF ORDER $v$ , $v = 0, 1$  |
| $K_v$  | - | MODIFIED BESSEL FUNCTION OF THE SECOND KIND OF ORDER $v$ , $v = 0, 1$   |
| $K_i$  | - | THERMAL CONDUCTIVITY OF THE POWER INSULATION OF THE ANNULUS, $\frac{\text{BTU}}{\text{HR} - \text{FT}^{\circ}\text{F}}$ |



|       |   |  |
|-------|---|--|
| $K_m$ | - | THERMAL CONDUCTIVITY OF THE METER BAR, $\frac{\text{BTU}}{\text{HR} - \text{FT}^\circ\text{F}}$        |
| $K_s$ | - | THERMAL CONDUCTIVITY OF THE SPECIMEN BAR, $\frac{\text{BTU}}{\text{HR} - \text{FT}^\circ\text{F}}$     |
| $L$   | - | LENGTH OF THE SPECIMEN BAR, FT   |
| $l$   | - | NON-DIMENSIONAL LENGTH OF THE SPECIMEN BAR, $\frac{L}{W}$  |
| $M$   | - | LENGTH OF THE METER BAR, FT  |
| $m$   | - | POSITIVE INTEGER   |
| $n$   | - | POSITIVE INTEGER   |
| $P$   | - | RADIAL HEAT FLOW THROUGH THE INNER CYLINDRICAL SURFACE OF THE ANNULUS, $\frac{\text{BTU}}{\text{HR}}$  |
| $p$   | - | NON-DIMENSIONAL RADIAL HEAT FLOW   |
| $Q$   | - | AXIAL HEAT FLOW, $\frac{\text{BTU}}{\text{HR}}$  |
| $Q_i$ | - | AXIAL HEAT FLOW THROUGH THE AXIAL PLANE AT POSITION $i$ IN THE CUT-BAR, $\frac{\text{BTU}}{\text{HR}}$ |
| $Q_T$ | - | TOTAL AXIAL HEAT FLOW WITH NO RADIAL LOSSES, $\frac{\text{BTU}}{\text{HR}}$                            |
| $q$   | - | NON-DIMENSIONAL AXIAL HEAT FLOW  |
| $R$   | - | RESISTANCES, $\frac{\text{HR} - \text{FT}^\circ\text{F}}{\text{BTU}}$                                  |
| $r$   | - | RADIAL CYLINDRICAL COORDINATE VARIABLE, FT   |
| $S_m$ | - | TEMPERATURE GRADIENT IN THE METER-BAR, $\frac{^\circ\text{F}}{\text{FT}}$                              |
| $S_s$ | - | TEMPERATURE GRADIENT IN THE SPECIMEN BAR, $\frac{^\circ\text{F}}{\text{FT}}$                           |
| $S_i$ | - | TEMPERATURE GRADIENT AT POSITION $i$ IN THE CUT-BAR, $\frac{^\circ\text{F}}{\text{FT}}$                |

|            |   |  |
|------------|---|--|
| T          | - | TEMPERATURE AT THE SOURCE END OF THE APPARATUS, °F   |
| u          | - | NON-DIMENSIONAL AXIAL CYLINDRICAL COORDINATE VARIABLE  |
| V          | - | TEMPERATURE VARIABLE, °F   |
| w          | - | LENGTH OF THE CUT-BAR APPARATUS, FT  |
| Z          | - | AXIAL CYLINDER COORDINATE VARIABLE MEASURED FROM THE SOURCE END OF THE APPARATUS, FT           |
| $\alpha$   | - | CONSTANT   |
| $\gamma$   | - | NET FRACTION OF POWER LOST OR GAINED IN THE CUT-BAR BETWEEN, $u = 0$ and $u = u_1$             |
| $\theta$   | - | NON-DIMENSIONAL TEMPERATURE VARIABLE, $\frac{V - V_2}{V_1 - V_2}$                              |
| $\rho$     | - | NON-DIMENSIONAL RADIAL CYLINDRICAL COORDINATE VARIABLE, $\frac{r}{w}$                          |
| $\sigma_i$ | - | NON-DIMENSIONAL THERMAL CONDUCTIVITY OF THE POWER INSULATION OF THE ANNULUS, $\frac{K_i}{K_m}$ |
| $\sigma_s$ | - | NON-DIMENSIONAL THERMAL CONDUCTIVITY OF THE SPECIMEN BAR, $\frac{K_s}{K_m}$                    |
| $\psi_m$   | - | NON-DIMENSIONAL TEMPERATURE GRADIENT IN THE METER-BAR, $\frac{S_m w}{T}$                       |
| $\psi_s$   | - | NON-DIMENSIONAL TEMPERATURE GRADIENT IN THE SPECIMEN BAR, $\frac{S_s w}{T}$                    |
| $\Omega$   | - | NET FRACTION OF POWER LOST OR GAINED IN THE ANNULUS BETWEEN $u = 0$ and $u = u_1$              |

## I. INTRODUCTION

The "Cut-Bar" technique of measuring thermal conductivity is a steady state comparative method which is most accurate in the low and intermediate temperature ranges for highly conductive materials. The schematic of the elements of a typical apparatus is illustrated in Figure 1. It consists of a pair of meter bars or discs between which a specimen is interposed. This composite bar is surrounded by an annulus of powder insulation which, in turn, is encased in a heated metal cylinder acting as a guard against extraneous heat losses. An axial heat flux is established by an isothermal source and sink at either end of the assembly.

For a first approximation, the determination of the specimen's conductivity is rather straightforward. Fourier's equation is written once for the average of the meter bar values and once for the specimen:

$$Q/A|_m = K_m S_m \quad (1)$$

$$Q/A|_s = K_s S_s \quad (2)$$

where  $Q/A$  is the heat flux,  $k$  the thermal conductivity, and  $S$  the temperature gradient in the axial direction. By assuming the heat flow and cross-sectional areas constant throughout the composite bar the following relationship exists:

$$K_s = K_m [S_m/S_s] \quad (3)$$

where the temperature gradients are measured and the conductivity of the meter bar is known either by using a known standard material for the meter bar or by previous calibration with known standards as specimens.

Actually, the constant heat flow assumption is in error for two reasons; the radial heat exchange with the guard and the axial shunting exchange with the powder insulation caused by the difference in conductivities between the meter bars and specimen (Figure 2). A more realistic expression of the relative heat fluxes is:

$$K_m S_m (1-\gamma_m) = K_s S_s (1-\gamma_s) \quad (4)$$

where  $\gamma$  is the ratio of the heat flow crossing the interface of the bar and insulation to the longitudinal heat flow in the bar if there were no losses (value in the bar a differential distance from the source). The evaluation of  $\gamma$  for a particular set of conditions may be done either analytically or experimentally. This report is concerned with an analytical solution.

FIGURE 1.

3

CUT-BAR APPARATUS WITH A LINEAR GUARD  
MATCHED AT THE ENDS

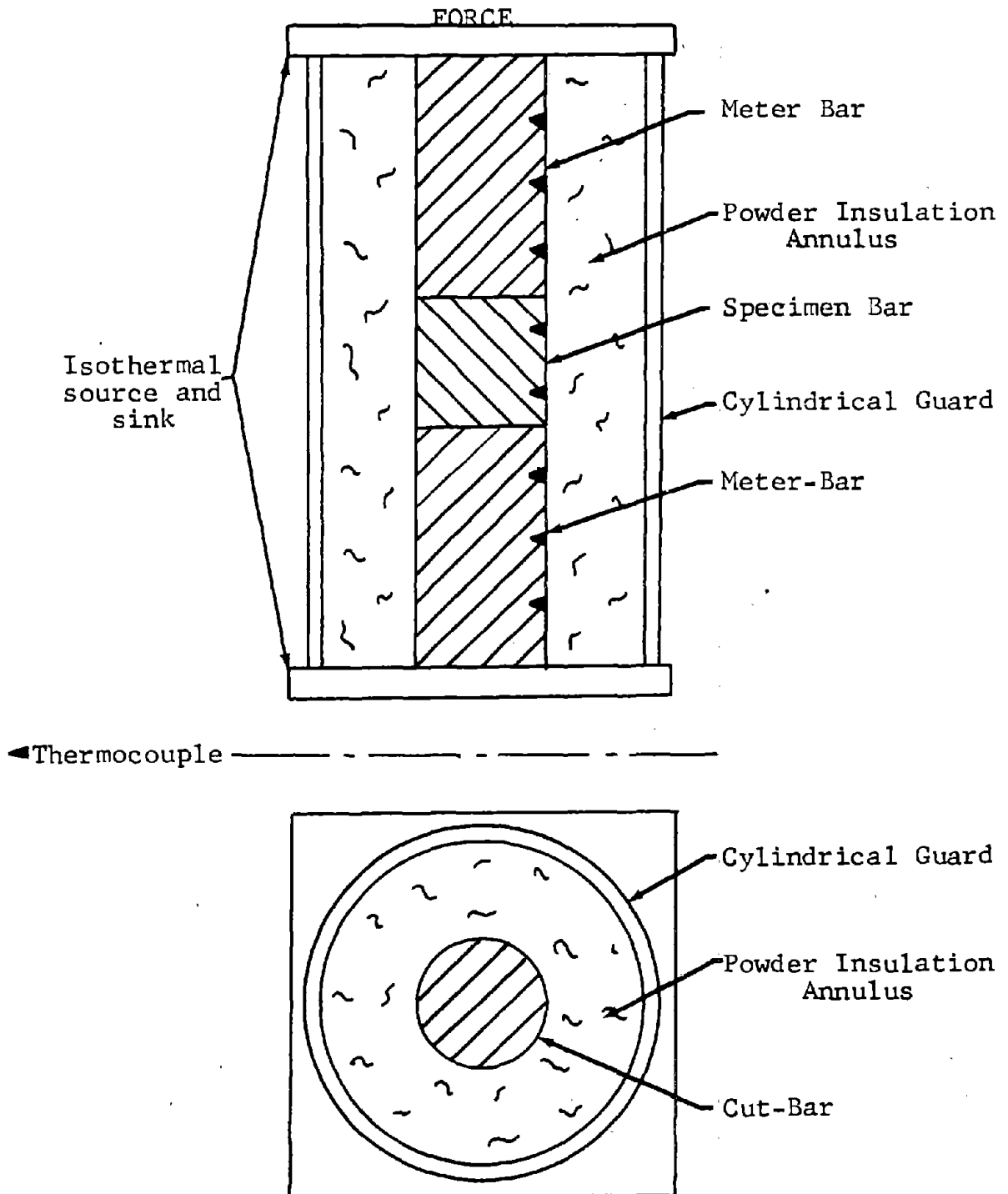
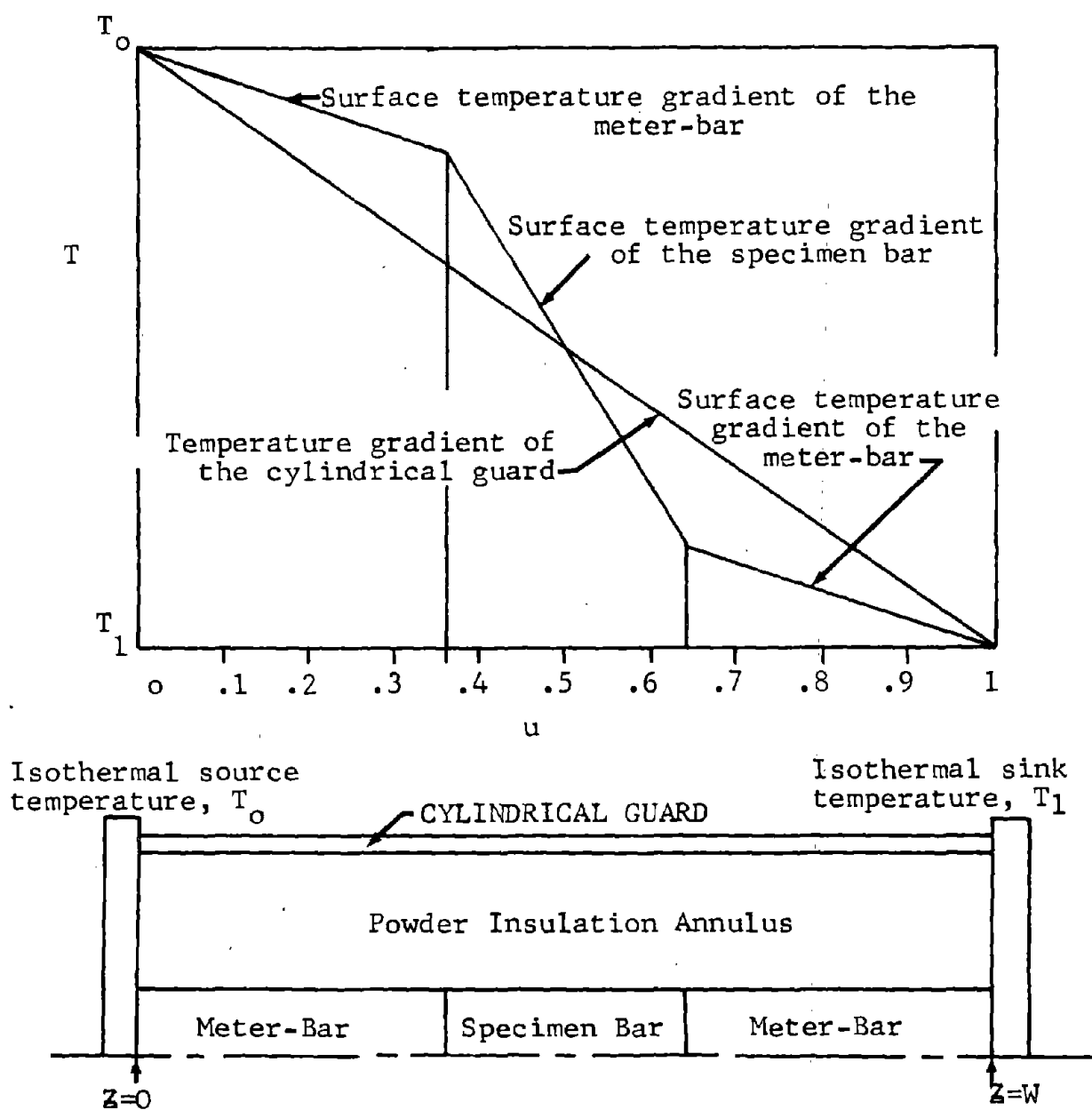


FIGURE 2

TEMPERATURES ON THE BOUNDARY SURFACES OF  
THE POWDER INSULATION ANNULUS



## II. ANALYSIS

A theoretical evaluation of  $\gamma$  may be obtained by determining the heat flow across the interface of the bar and powder insulation. The heat conduction equation and boundary conditions for the annulus of insulation are assumed to be:

$$\frac{\partial^2 \theta}{\partial \rho^2} + \frac{1}{\rho} \frac{\partial \theta}{\partial \rho} + \frac{\partial^2 \theta}{\partial \mu^2} = 0 \quad (5)$$

$$\left. \begin{array}{ll} \rho = a & \theta = \frac{G(z) - v_2}{v_1 - v_2} \\ \rho = b & \theta = \frac{H(z) - v_2}{v_1 - v_2} \\ \mu = 0 & \theta = 1 \\ \mu = 1 & \theta = 0 \end{array} \right\} \quad (6)$$

Where the notation may be realized by reference to Figure 3 and the nomenclature section. The general solution to equation (5) is of course known (Reference [1]) and when applied to the particular boundary conditions the temperature distribution throughout the insulation is obtained. This distribution expression may be differentiated to obtain the radial gradient which in turn may be evaluated at the A radius boundary and then integrated along the A axis to get the total heat flow crossing the bar-insulation interface. Dividing this result by the longitudinal heat flow in the bar (assuming no losses) results in the following expression:

$$\gamma = k_i \left( \frac{1}{k_m} - \frac{1}{k_s} \right) \frac{2w}{\pi^2 A} \sum_{m=1}^{\infty} (-1)^m \left( \frac{1 - \cos(2m\pi z)}{2m} \right) \sin \left( \frac{m\pi L}{w} \right) \quad (7)$$

$$\left[ \frac{K_o \left( \frac{2m\pi B}{w} \right) I_1 \left( \frac{2m\pi A}{w} \right)}{k_o \left( \frac{2m\pi B}{w} \right) I_o \left( \frac{2m\pi A}{w} \right)} + \frac{K_1 \left( \frac{2m\pi A}{w} \right) I_o \left( \frac{2m\pi B}{w} \right)}{K_o \left( \frac{2m\pi A}{w} \right) I_o \left( \frac{2m\pi B}{w} \right)} \right]$$

where the complete details of the above mentioned steps are presented in Appendix A. Equation (7) may be separated into two terms of independent physical meaning, the conductivity and geometrical factors:

$$F_k = \left( k_i \frac{1}{k_m} - \frac{1}{k_s} \right) \quad (8)$$

$$F_g = \frac{2w}{\pi^2 A} \sum_{m=1}^{\infty} (-1)^m \left( \frac{1 - \cos(2m\pi Z)}{2m} \right) \sin \left( \frac{m\pi L}{w} \right) \left[ \frac{K_o \left( \frac{2m\pi B}{w} \right) I_1 \left( \frac{2m\pi A}{w} \right) + K_1 \left( \frac{2m\pi A}{w} \right) I_o \left( \frac{2m\pi B}{w} \right)}{K_o \left( \frac{2m\pi B}{w} \right) I_o \left( \frac{2m\pi A}{w} \right) + K_o \left( \frac{2m\pi A}{w} \right) I_o \left( \frac{2m\pi B}{w} \right)} \right] \quad (9)$$

Thus

$$\gamma = F_k \cdot F_g \quad (10)$$

Because of its complexity equation (9) has been programmed and is usually found to converge on a sufficiently accurate value in less than 150 terms. The flow chart and programs are presented in Appendix B. For a given apparatus  $F_g$  is seen to be a function of  $z$  only. However since the specimen length ( $L$ ) effects the overall length ( $w$ ) the actual values of  $F_g(z)$  must be determined for each test. In Figure 4 a curve for particular inputs of  $w = 9.5$  inches,  $A = 1$  inch,  $B = 3$  inches,  $L = 2$  inches, represents the variation of the geometrical factor ( $F_g$ ) with dimensionless distance ( $\mu$ ).

A reproduction of the computer program output can be seen in Figure 5 for one-half of the cut-bar. Since the ends of the cut-bar and guard are matched, the radial losses and gains are symmetrical about the center of the apparatus; the geometrical factor  $F_g(Z)$  plotted over one-half of the cut-bar is a mirror image for the other half.

Finding  $F_k$  for the apparatus from equation (8) and using  $F_g(Z)$  from the computer, the same curve with different ordinate scale will represent  $\gamma (Z)$ .



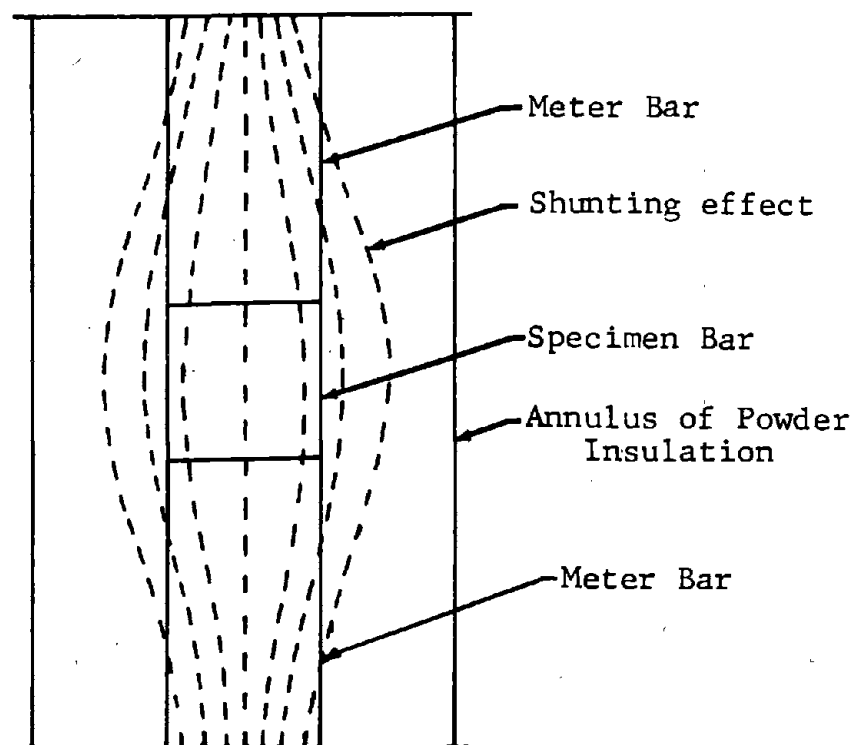
In an earlier work (Reference 2), Flynn carried out an analysis for the case of the outer boundary temperature distribution equal to the inner boundary; that is,  $H(Z) = G(Z)$ . A comparison with this ideal case is made in Figure 6. The cut-bar apparatus with a matched guard has smaller geometrical factors compared with a similar apparatus and a linear guard matched at the ends, (Figure 6). The two cut-bar apparatus have the same dimensionless ratios,  $\frac{L}{W} = 3$  and  $\frac{L}{A} = 4$ , and differ only in the thermal guarding. The relative flatness of the matched guard's correction curves, has the advantage of not having to average the correction factor between thermocouples discussed in the example in Chapter III. Furthermore, as the ratio  $\frac{B}{A}$  decreases in the linear guard apparatus, the geometrical factor will increase to a very large number. Conversely, letting  $\frac{B}{A}$  decrease in the matched guard apparatus, the geometrical factor will decrease, and in the limit as  $\frac{B}{A}$  approaches one,  $F_g$  approaches zero. These phenomena are better illustrated in Figure 7, which is a plot of the maximum geometrical factors (at the mid-horizontal plane) against the ratio of the guard and bar radii. The linear guard's increasing geometrical factor with decrease of  $\frac{B}{A}$  may be explained with the decreasing insulating resistance, the radial losses begin to approach the axial flux. The matched guard apparatus has a minimum of radial losses; thus, letting  $\frac{B}{A} \rightarrow 1$  decreases the shunting loss by decreasing the medium through which it takes place. The conditions of the zero limit are, of course, quite impractical.

It may be concluded that although the errors associated with the linear guard are of greater magnitude and variation along the longitudinal axis, than that for a matched guard, they are not excessive for large  $\frac{B}{A}$  ratios. Consequently, this method may still be the preferred technique; particularly, when considering the additional complexity and cost of the matched guard's experimental apparatus. The details of how to design and correct a linear guard apparatus are discussed in Chapter III.

FIGURE 3

SHUNTING OF HEAT FLUX IN A  
CUT-BAR APPARATUS

Sink at Temperature,  $V_2$



Source at Temperature,  $V_1$

FIGURE 4

19

PLOT OF THE GEOMETRICAL FACTOR ON THE LEFT SCALE AND FRACTIONAL POWER CHANGE ON THE RIGHT SCALE OF THE ORDINATE AXIS VERSUS THE DIMENSIONLESS LENGTH  $u$  ON THE AXIS OF THE ABSCISSA

Dimensionless parameters for this apparatus are:

$$\frac{L}{A} = 2., \frac{L}{W} = .2105, \frac{B}{A} = 3., \frac{K_1}{K_s} = .01111, \frac{K_1}{K_m} = .001111$$

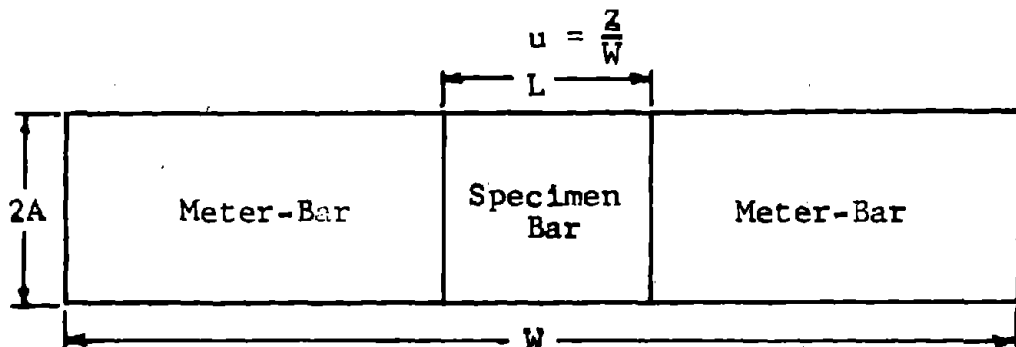
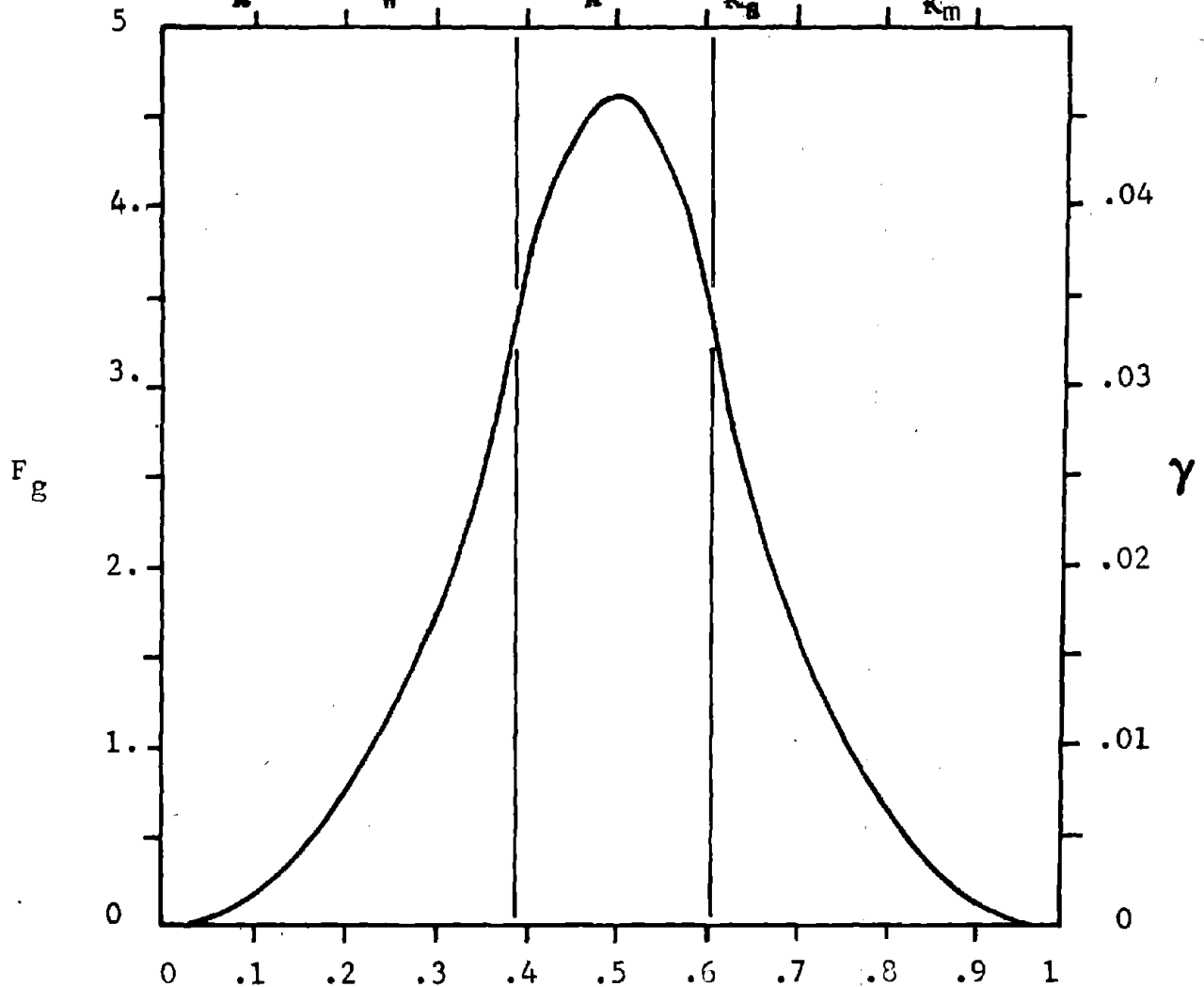


FIGURE 5

10

COMPUTER OUTPUT

RESULTS OF POWER LOSS OVER LENGTH OF METER-BAR

$F_g$  VERSUS  $Z$  FOR 20 POINTS FROM  $Z=0$  TO END

| <u>W</u> | <u>A</u> | <u>B</u> | <u>L</u> | <u>TEST</u> | <u>P</u> | <u>M</u> | <u>F</u> |
|----------|----------|----------|----------|-------------|----------|----------|----------|
| 9.50000  | 1.00000  | 3.00000  | 2.00000  | .00010      | 20       | 150      | 19       |

| <u>POINT</u> | <u>Z</u> | <u>KL</u> | <u>SER</u> | <u><math>F_g</math></u> | <u>M=150</u> |
|--------------|----------|-----------|------------|-------------------------|--------------|
| 1            | .23750   | 3         | .0057214   | .0110143                |              |
| 2            | .47500   | 59        | .0228464   | .0439817                |              |
| 3            | .71250   | 3         | .0514361   | .0990198                |              |
| 4            | .95000   | 3         | .0915257   | .1761964                |              |
| 5            | 1.18750  | 21        | .1433035   | .2758740                |              |
| 6            | 1.42500  | 3         | .2069009   | .3983055                |              |
| 7            | 1.66250  | 21        | .2825233   | .5438862                |              |
| 8            | 1.90000  | 3         | .3706142   | .7134703                |              |
| 9            | 2.13750  | 21        | .4717329   | .9081341                |              |
| 10           | 2.23750  | 21        | .5867708   | 1.1295939               |              |
| 11           | 2.61250  | 21        | .7170570   | 1.3804081               |              |
| 12           | 2.85000  | 3         | .8646966   | 1.6646296               |              |
| 13           | 3.08750  | 1         | 1.0334212  | 1.9894417               |              |
| 14           | 3.32500  | 2         | 1.2303858  | 2.3686188               |              |
| 15           | 3.56250  | 0         | 1.4725646  | 2.8348377               |              |
| 16           | 3.80000  | 0         | 1.8485560  | 3.5586596               |              |
| 17           | 4.03750  | 0         | 2.1179562  | 4.0772827               |              |
| 18           | 4.27500  | 2         | 2.2792856  | 4.3878582               |              |
| 19           | 4.51250  | 0         | 2.3698414  | 4.5621874               |              |
| 20           | 4.75000  | 2         | 2.3992300  | 4.6187635               |              |

**FIGURE 6**  
**COMPARISON OF THE GEOMETRICAL FACTORS FOR A CUT-BAR**  
**APPARATUS HAVING A MATCHED GUARD WITH AN APPARATUS**  
**HAVING A LINEAR GUARD MATCHED AT THE ENDS**

The dimensionless variables of the  
apparatus are:  $\frac{L}{W} = 3$ ,  $\frac{L}{A} = 4$

L. G. - Linear guard matched at the ends  
M. G. - Matched Guard

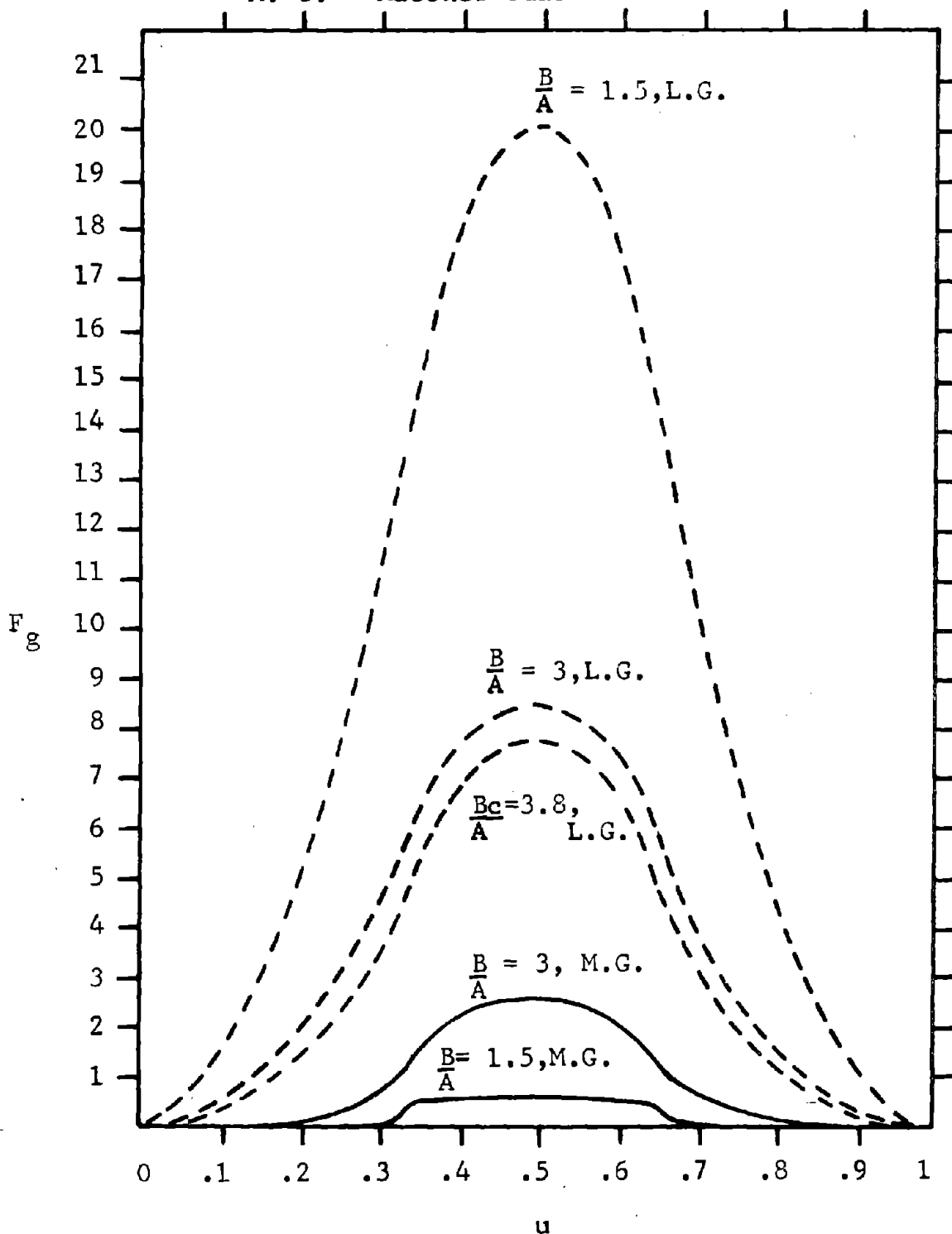
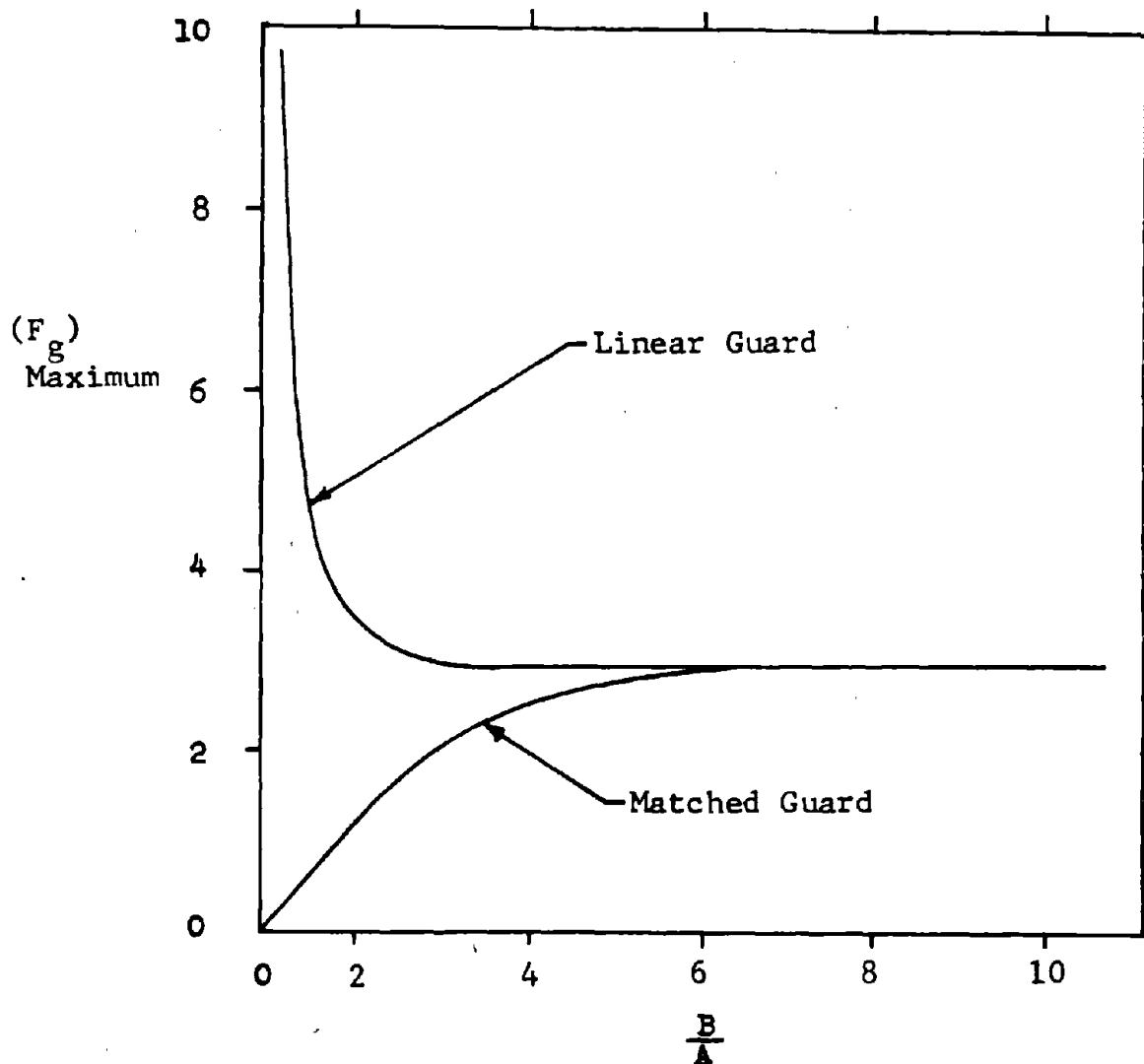


FIGURE 7

GEOMETRICAL FACTOR AS A FUNCTION OF THE RATIO  
OF APPARATUS DIAMETERS

Plot of the geometrical factor as a function of  
the ratio of guard and specimen diameters for a  
matched guard and a linear guard matched at ends.



### III. DESIGN

The computer results of equation (9) are also plotted as design charts. The design charts can be used to find optimum dimensions for a test setup. A larger than practical range of variables are shown, so that the designer can be sure of an optimum. It should be noted that in the development of the design charts, the only dimensionless parameters are those with physical implications.

The design chart (Figure 8) plots the geometrical factor  $F_g$  against the radii ratio of guard to bar  $\frac{B}{A}$ , using specimen length to specimen radius  $\frac{L}{A}$ , and overall length  $\frac{L}{w}$ , as parameters. The geometrical factor  $F_g$ , should be kept to a minimum to obtain the optimum design. It is evident from equation (9) that as  $\frac{B}{A}$  approaches 1,  $F_g$  approaches infinity as a limit for any  $\frac{L}{A}$  and  $\frac{L}{w}$ . However, as  $\frac{B}{A}$  increases  $F_g$  rapidly settles down to various asymptotic values. An arbitrary curve designated  $B_c$  is drawn from a locus of points in the family of curves for  $\frac{L}{A}$  and  $\frac{L}{w}$  where the slope of these curves have an absolute value of 0.01. An increase in the ratio  $\frac{B}{A}$ , passed the ratio  $\frac{B_c}{A}$  does not significantly decrease  $F_g$ . Thus,  $\frac{B_c}{A}$  may be considered as points of diminishing return and are the recommended value for optimum design.

Figure 9 is a plot of  $F_g$  against  $\frac{L}{w}$  for an  $\frac{L}{A}$  family of curves. It also has a scale on the right ordinate of  $\frac{B_c}{A}$ . If the designer uses  $\frac{B_c}{A}$  as the sizing of the annulus, he may immediately find the minimum geometrical factor  $F_g$ , for whatever values of  $\frac{L}{w}$  and  $\frac{L}{A}$  he desires. It may be seen in Figure 9, that as  $\frac{L}{w}$  approaches the limit  $\frac{L}{w} = 1$ ,  $F_g \rightarrow 0$  for all values of  $\frac{L}{A}$ . When  $\frac{L}{w} = 1$ , the cut-bar is a solid bar composed of the specimen material; similarly, when  $L = 0$ , the cut-bar is a solid bar, but composed of meter bar material. In both cases, there is an axial temperature gradient in the cut-bar which matches the axial temperature gradient in the guard. Therefore,  $F_g$  must be zero, because there is neither a radial heat flow nor a shunting flow in the annulus.

The effect of varying the specimen thermal conductivity on the thermal conductivity factor,  $F_k$ , (Figure 10) can be seen by using equation (8) to plot  $F_k$  against  $\frac{K_s}{K_i}$  for various ratios of  $\frac{K_m}{K_i}$ . The plotted quantities go through zero at  $\frac{K_s}{K_i} = \frac{K_m}{K_i}$ , then approach  $\infty$  as  $\frac{K_s}{K_i}$  becomes small, and asymptotically approach  $-\frac{K_i}{K_m}$  as  $\frac{K_s}{K_i}$  becomes large.

Since a designer would choose a geometrical factor which would be small, he could multiply the ordinary scale of Figure 10 to obtain  $\gamma$ . The ordinate would be the measure of thermal conductivity of materials in terms of fractional power gained or lost in the cut-bar apparatus.

If it is necessary to measure a large range of specimen thermal conductivities with a single pair of meter-bars, the conductivity of the meter-bar should be in the lower end of the range. To have a minimal thermal conductivity factor range, for a given range of specimen materials using only a single pair of meter-bars, it is necessary to find the arithmetic average of the resistance of the specimen range. The arithmetic average of the maximum and minimum of the specimen resistance range will be used as the optimum resistance for the meter-bar.

Therefore,

$$R_m = 1/2 \left[ (R_s)_{\max} + (R_s)_{\min} \right] \quad (11)$$

Substituting the equivalent thermal conductivity for resistance, that is,  $R = \frac{1}{K}$ , into equation (11) it becomes,

$$K_m = \frac{2 (K_s)_{\max} (K_s)_{\min}}{(K_s)_{\max} + (K_s)_{\min}} \quad (12)$$

$(K_s)_{\max}$  and  $(K_s)_{\min}$  are the maximum and minimum specimen thermal conductivities to be measured.

The maximum fractional power is approximately,

$$\gamma_{\max} = \pm \frac{K_i}{2} \left[ \frac{1}{(K_s)_{\min}} - \frac{1}{(K_s)_{\max}} \right] F_g \quad (13)$$

When  $(K_s)_{\max}$  is very large relative to  $(K_s)_{\min}$ , equation (12) is approximately,

$$K_m = 2 (K_s)_{\min} \quad (14)$$

For the maximum fractional power change over the range, equation (13) becomes,

$$\gamma_{\max} = \pm \frac{K_i}{2 (K_s)_{\min}} F_g \quad (15)$$



Figure 11 shows the table with several ranges of thermal conductivity; the preferred meter-bar for each range, and the maximum fractional power change associated for a given geometrical factor of 1.0, and an insulation thermal conductivity of

$$.058 \frac{\text{BTU}}{\text{HR-FT}^2\text{F}} .$$

To illustrate the fractional power change that would arise if a range of materials for the specimen bar were measured using the same meter-bar and insulation annulus,  $\gamma$  is plotted against dimensionless length in Figure 12. The geometrical dimensions of the cut-bar apparatus in Figure 12 are the dimensions used for the  $F_g$  values to obtain a plot of  $\gamma$  versus the dimensionless length  $u$ . The quantity  $\gamma(u)$  is shown for specimens having a thermal conductivity ranging from one-tenth to ten times that of the meters.

The following is an example problem, illustrating the use of the design charts and equations of a cut-bar apparatus having an optimal design using a minimal fractional power change. The fractional power change is dependent on both the geometrical factor and the thermal conductivity factor, while the geometrical and thermal conductivity factors are independent of one another. Thus, these factors are each minimized separately.

Assuming that the particular design requirements are limited to an overall length of  $w$  equal to 9.5 inches, with the specimen dimensions of length  $L$  equal to 2 inches, and specimen radius  $A$  equal to 1 inch, the specimen thermal conductivity will have a range from a minimum of  $4.5 \frac{\text{BTU}}{\text{HR-FT}^2\text{F}}$  to a maximum of  $242 \frac{\text{BTU}}{\text{HR-FT}^2\text{F}}$  (the range of most metals).

From the above known dimensions:  $\frac{L}{A} = 2$  and  $\frac{L}{W} = .2111$ . The design chart in Figure 9 indicates the dimensionless ratio  $\frac{B_c}{A}$  is found to be  $\frac{B_c}{A} = 4.06$  or  $B_c = 4.06$  inches. Thus, the guard diameter should be at least 4 inches or greater.

The computer program in Appendix B is used to calculate the geometrical factor for 20 points along the cut-bar. The computer program stops when the geometrical factor has converged within the test range of .0001 or reaches the maximum number of series terms of  $M$  equal to 150. The frequency  $F$  of the test for convergency occurs every 7 terms in the series.

The inputs into the computer program are:  $W = 9.5$  inches;  $A = 1.0$  inch;  $B = 4.06$  inches;  $L = 2.0$  inches; Test = .0001;  $P = 20$  points;  $M = 150$

terms, and  $F = 7$ . The resulting output from the computer program is illustrated in Figure 13. Calculated for each point is the distance  $Z$  of that point in inches from the reference end, the number of KL terms before the last term in the series is calculated, the value of the SER series summation, and the value for the geometrical factor  $F_g$ . The resulting output for 20 points along one symmetrical half of the cut-bar is presented in Figure 13. From this output of the computer program, a graph (Figure 14) is drawn for  $F_g$  versus  $Z$ . In Figure 14,  $F_g$  is on the left scale of the ordinate axis and its maximum value at the center of the cut-bar is 4.31.

Since the apparatus is to be used to measure the thermal conductivity of specimens ranging from Bismuth to that of Silver, the limiting conductivity values are  $(K_s)_{\min} = 4.5 \frac{\text{BTU}}{\text{HR-FT}^2\text{F}}$  and  $(K_s)_{\max} = 242 \frac{\text{BTU}}{\text{HR-FT}^2\text{F}}$ . The insulation best suited for the apparatus has a value of  $K_i = .1 \frac{\text{BTU}}{\text{HR-FT}^2\text{F}}$ . Using equation (12),  $K_m$  is calculated as  $9 \frac{\text{BTU}}{\text{HR-FT}^2\text{F}}$ , which is in the range of stainless steels. Using the above values for  $K_i$ ,  $(K_s)_{\min}$ ,  $(K_s)_{\max}$  and  $(F_g)_{\max}$  and substituting these values into equation (13), the maximum value of the fractional power change is  $-.047$  which is at the center of the specimen bar.

To calculate the fractional power change for a specific test the apparent conductivity is first used, for instance  $K_s = 90 \frac{\text{BTU}}{\text{HR-FT}^2\text{F}}$ . Knowing  $K_i$  and  $K_m$  the conductivity factor  $F_k$  is found to be .01 from equation (8). Since the geometrical factor has been plotted for the apparatus in Figure 14, the fractional power change can be found by changing the scale on the axis of the ordinate by a factor of .01, and this scale is shown on the right scale on the axis of the ordinate.

Since the temperature gradients are calculated between two thermocouples placed a finite distance apart, the fractional power changes  $\gamma_m$  and  $\gamma_s$  which are used in equation (4) represent the average fractional power changes between the measuring stations, this average  $\gamma$  can be calculated as,

$$\gamma_{\text{aver}} = \frac{\int_{Z_1}^{Z_2} \gamma dZ}{Z_2 - Z_1}$$

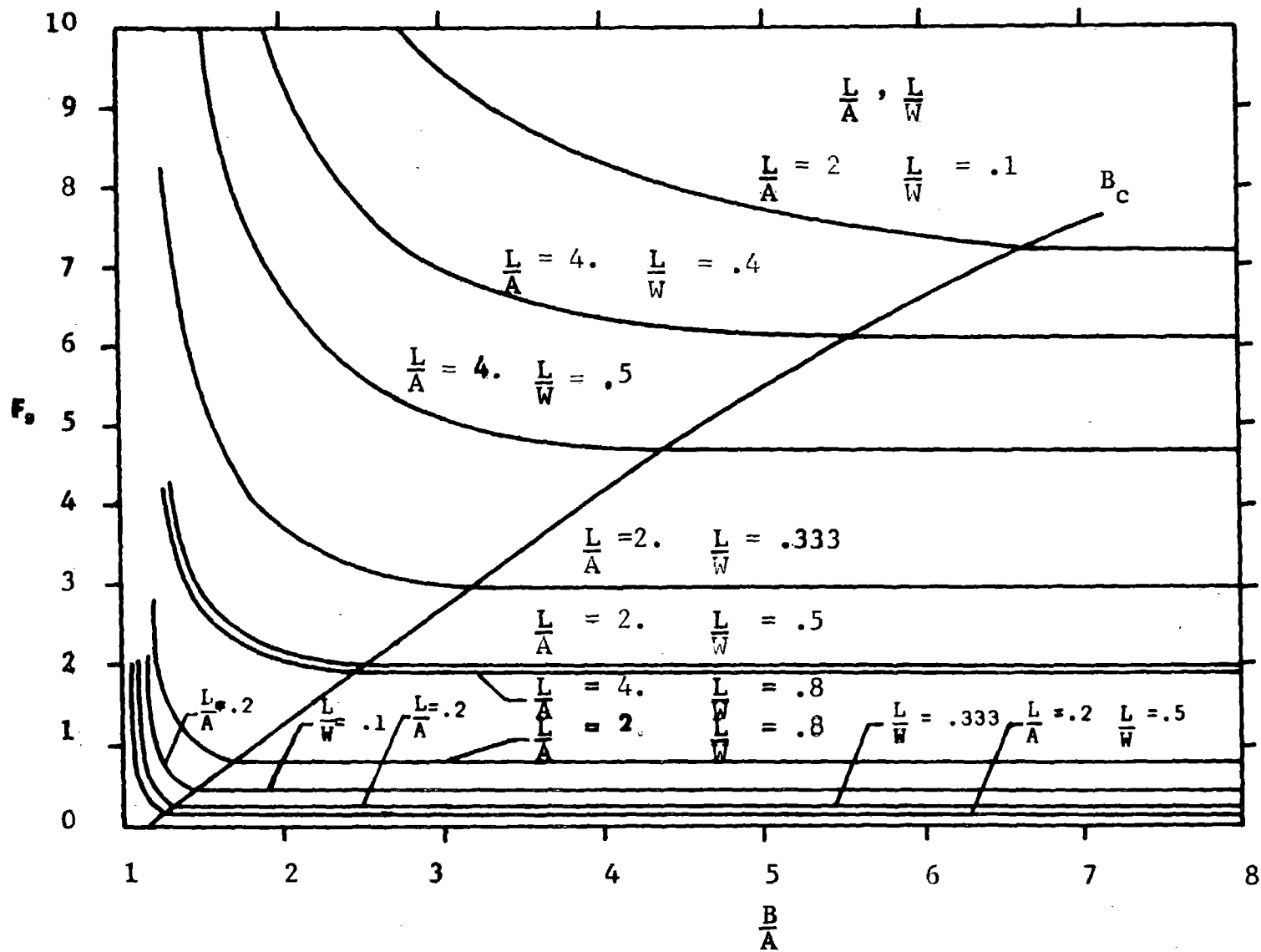
To find the average  $\gamma$  to be used for  $\gamma_m$  in this example, (referring to Figure 14) the cross-hatched area under the curve from  $Z_1 = 1.1875$  to  $Z_2 = 3.325$  inches, is measured by counting graph squares with the result that  $\gamma_m = .01025$ .

$\gamma_s$  is calculated by using the same graphical procedure with the two measuring thermocouples being at points  $Z_1 = 4.037$  and  $Z_2 = 5.463$  on the specimen bar; thus  $\gamma_s$  is .0414.

The fractional power change for  $\gamma_m$  and  $\gamma_s$  is then substituted into equation (4), where  $K_m = 9 \frac{\text{BTU}}{\text{HR-FT}^2\text{F}}$ . The resulting equation, to find the thermal conductivity of the specimen for the example problem, is,

$$K_s = 8.72 \frac{S_m}{S_s}$$

$S_m$  and  $S_s$  are determined from the measurements of the thermocouples.

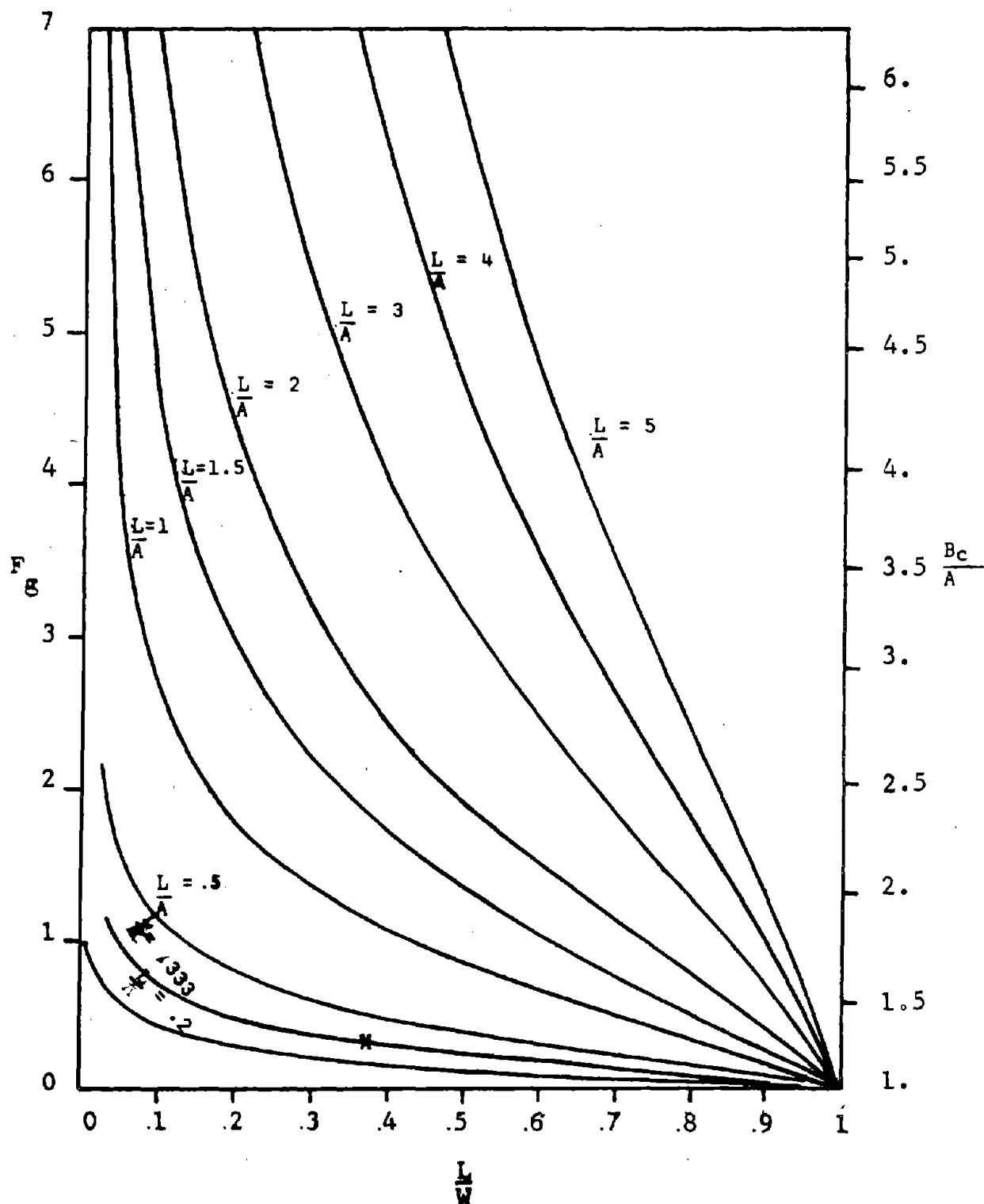


DESIGN CHART

FIGURE 8

FIGURE 9

DESIGN CHART FOR THE OPTIMUM DIMENSIONLESS

RATIO  $\frac{B}{A}$ , VARYING THE DIMENSIONLESSVARIABLES  $\frac{L}{A}$  AND  $\frac{L}{W}$ 

EFFECT OF SPECIMEN THERMAL CONDUCTIVITY ON THE  
THERMAL CONDUCTIVITY FACTOR FOR A RANGE OF  
DIMENSIONLESS RATIOS

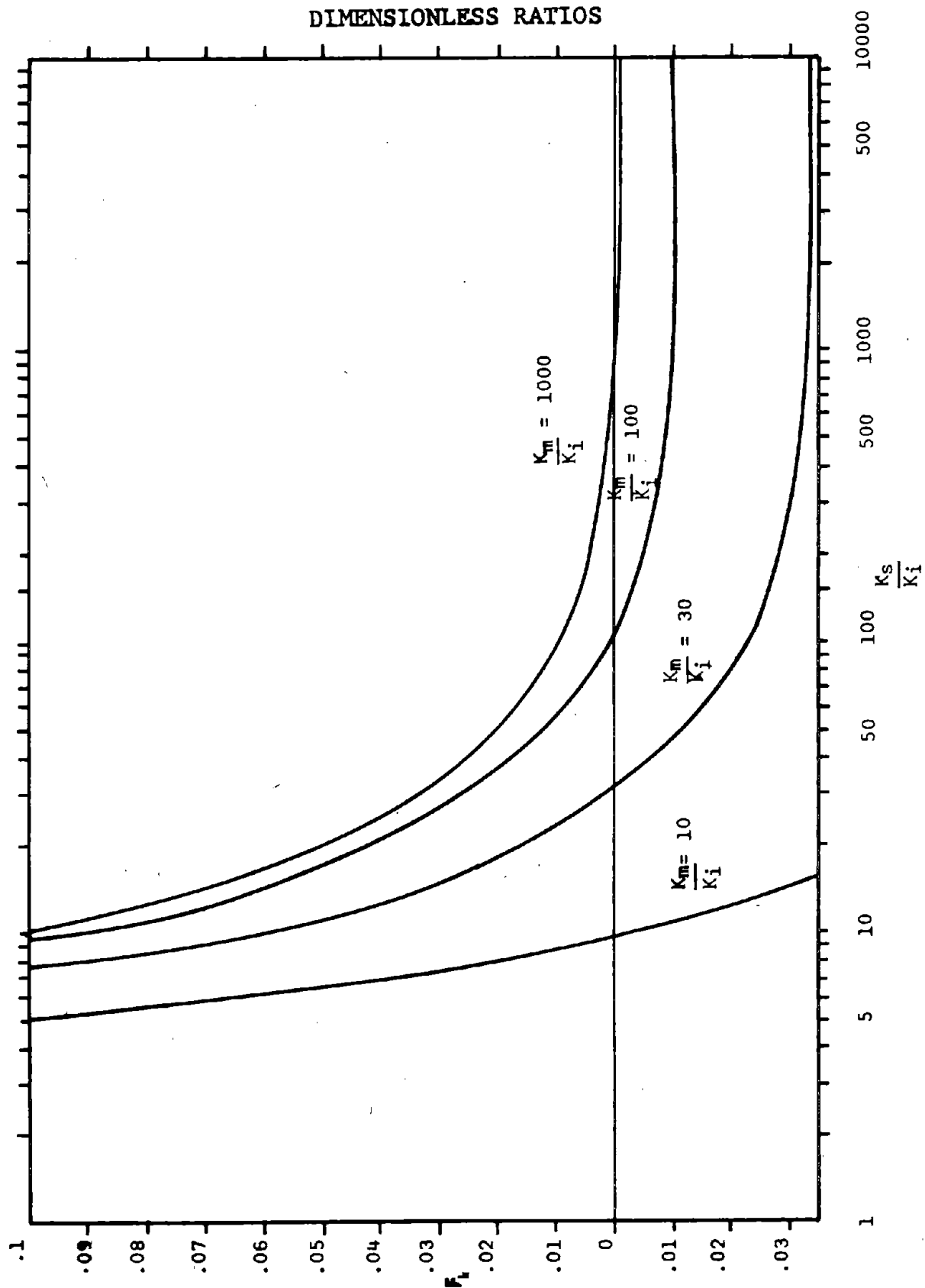


FIGURE 11

MAXIMUM ERRORS FOR VARIOUS RANGES OF  
SPECIMEN THERMAL CONDUCTIVITY

| Minimum                                     | Maximum                                     | Optimal $K_m$                               | Maximum Error<br>in $K_s$ Range |
|---|---|---|---------------------------------|
| $\frac{\text{BTU}}{\text{HR-FT}^2\text{F}}$ | $\frac{\text{BTU}}{\text{HR-FT}^2\text{F}}$ | $\frac{\text{BTU}}{\text{HR-FT}^2\text{F}}$ | + %<br>- %                      |
| 0.2889                                      | 0.5779                                      | 0.3872                                      | 5.0                             |
| .5779                                       | .8669                                       | .6935                                       | 1.7                             |
| .5779                                       | 1.1558                                      | .7686                                       | 2.5                             |
| .5779                                       | 2.8896                                      | .9651                                       | 4.0                             |
| .5779                                       | 5.7793                                      | 1.0518                                      | 4.5                             |
| .5779                                       | 57.7934                                     | 1.1443                                      | 5.0                             |
| 2.8896                                      | 5.7793                                      | 3.8548                                      | .50                             |
| 2.8896                                      | 28.8967                                     | 5.2534                                      | .90                             |
| 5.7793                                      | 28.8967                                     | 9.0753                                      | .40                             |
| 5.7793                                      | 57.7934                                     | 10.5183                                     | .45                             |
| 5.7793                                      | 577.9340                                    | 11.4430                                     | .50                             |
| 57.7934                                     | 577.9340                                    | 105.1839                                    | .045                            |

PLOT OF FRACTIONAL POWER CHANGE FOR A RANGE OF SPECIMEN  
THERMAL CONDUCTIVITIES VERSUS DIMENSIONLESS LENGTH

Dimensionless parameters for this  
apparatus are:  $\frac{L}{A} = 2$ ;  $\frac{L}{W} = .2105$ ;  $\frac{B}{A} = 3$

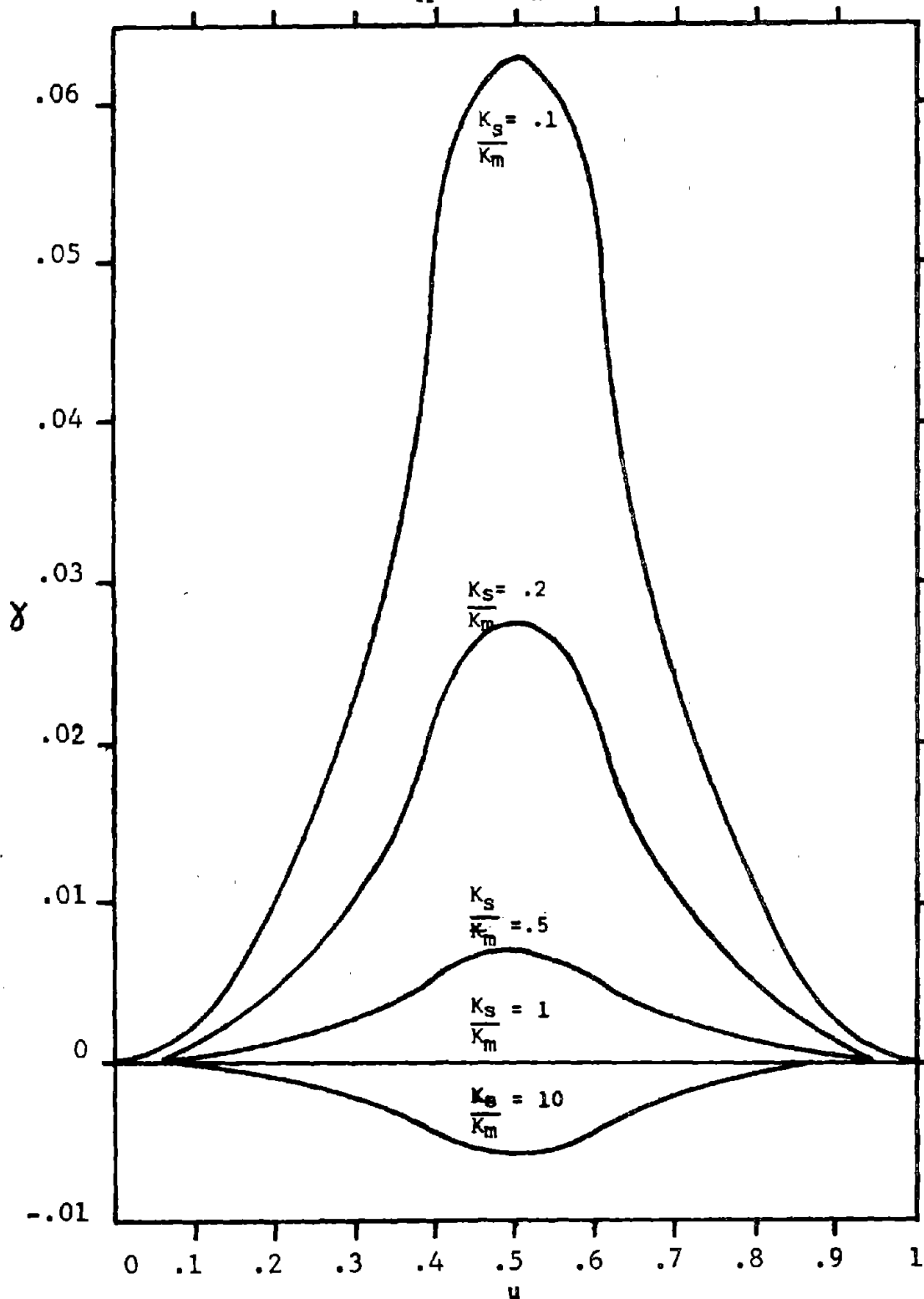




FIGURE 13  
COMPUTER OUTPUT

RESULTS OF POWER LOSS OVER LENGTH OF METER-BAR

$F_g$  VERSUS Z FOR 20 POINTS FROM Z=0 TO END

|          |          |          |          |             |          |          |          |
|----------|----------|----------|----------|-------------|----------|----------|----------|
| <u>W</u> | <u>A</u> | <u>B</u> | <u>L</u> | <u>TEST</u> | <u>P</u> | <u>M</u> | <u>F</u> |
| 9.50000  | 1.00000  | 4.06000  | 2.00000  | .00010      | 20       | 150      | 7        |

| <u>POINT</u> | <u>Z</u> | <u>KL</u> | <u>SER</u> | <u><math>F_g</math></u> | <u>M=150</u> |
|--------------|----------|-----------|------------|-------------------------|--------------|
| 1            | .23750   | 56        | .0047517   | .0091476                |              |
| 2            | .47500   | 35        | .0193526   | .0372558                |              |
| 3            | .71250   | 49        | .0436508   | .0840324                |              |
| 4            | .95000   | 35        | .0778525   | .1498741                |              |
| 5            | 1.18750  | 35        | .1221891   | .2352265                |              |
| 6            | 1.42500  | 35        | .1769584   | .3406630                |              |
| 7            | 1.66250  | 21        | .2425952   | .4670207                |              |
| 8            | 1.90000  | 42        | .3197168   | .6154876                |              |
| 9            | 2.13750  | 42        | .4089831   | .7873344                |              |
| 10           | 2.37500  | 21        | .5115743   | .9848330                |              |
| 11           | 2.61250  | 49        | .6291793   | 1.2112346               |              |
| 12           | 2.85000  | 21        | .7643035   | 1.4713626               |              |
| 13           | 3.08750  | 7         | .9209332   | 1.7728908               |              |
| 14           | 3.32500  | 2         | 1.1064501  | 2.1300297               |              |
| 15           | 3.56250  | 1         | 1.3382798  | 2.5763256               |              |
| 16           | 3.80000  | 0         | 1.7053046  | 3.2828861               |              |
| 17           | 4.03750  | 0         | 1.9674043  | 3.7874549               |              |
| 18           | 4.27500  | 2         | 2.1233365  | 4.0876404               |              |
| 19           | 4.51250  | 3         | 2.2105791  | 4.2555913               |              |
| 20           | 4.75000  | 7         | 2.2389335  | 4.3101764               |              |

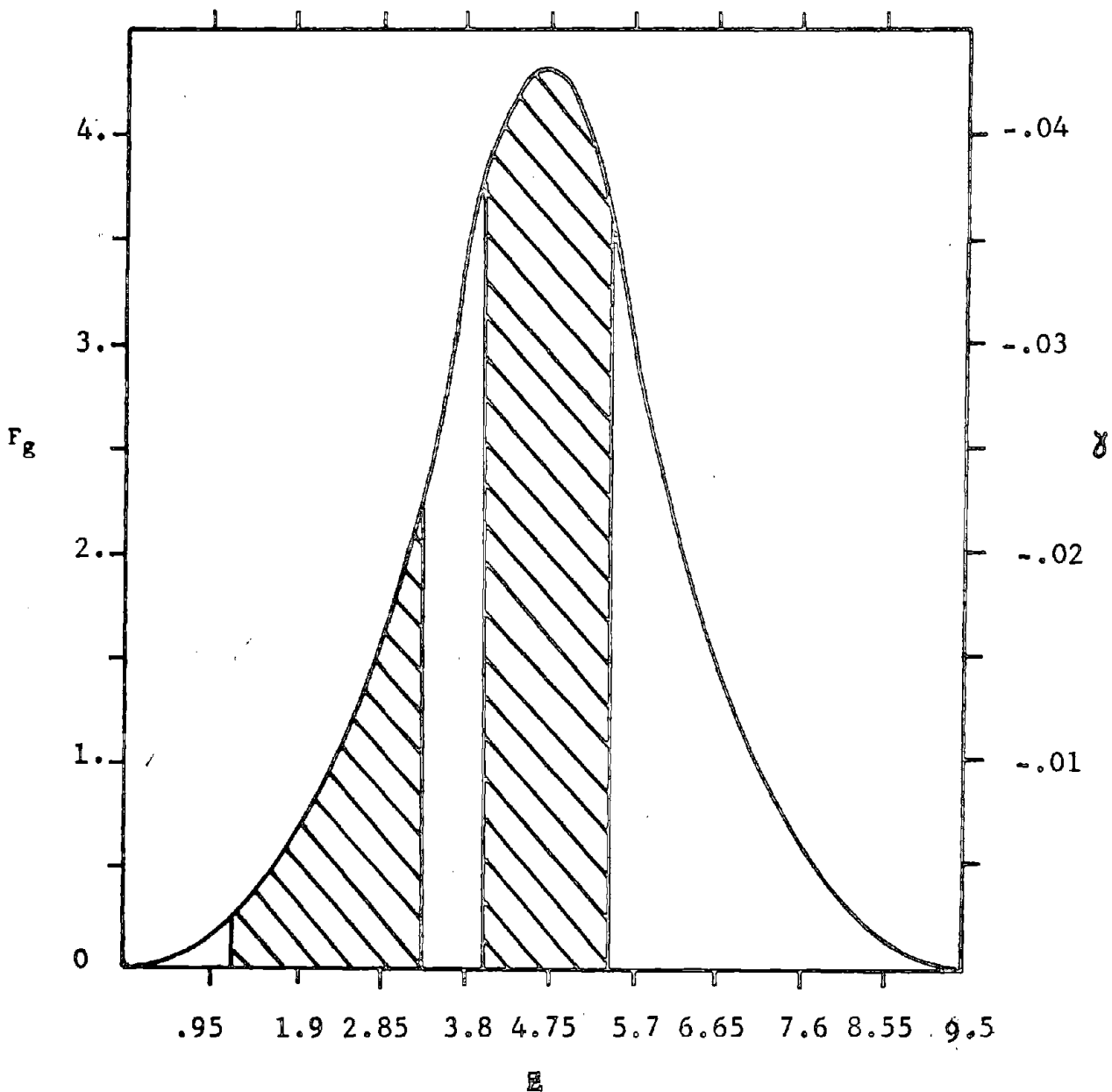
FIGURE 14

PLOT OF THE GEOMETRICAL FACTOR ON THE LEFT SCALE AND FRACTIONAL POWER CHANGE ON THE RIGHT SCALE OF THE ORDINATE AXIS VERSUS THE Z ON THE AXIS OF THE ABSCISSA

Dimensions of this apparatus are:

$$W = 9.5 \text{ in.}, A = 1 \text{ in.}, B = 4.06 \text{ in.}, L = 2 \text{ in.},$$

$$K_i = .01 \frac{\text{BTU}}{\text{HR-FT}^2\text{OF}}, K_s = 90 \frac{\text{BTU}}{\text{HR-FT}^2\text{OF}}, K_m = 9 \frac{\text{BTU}}{\text{HR-FT}^2\text{OF}}$$



#### IV. REFERENCES

- [1] Carslaw and Jaeger. Conduction of Heat in Solids. Second Edition. London: Oxford University Press, 1959, pp. 214-229.
- [2] Flynn, D. R. "Thermal Guarding of Cut-Bar Apparatus." Technical notes of the Conference on Thermal Conductivity Methods. Battelle Memorial Institute, Columbus, Ohio. October 26, 27, 28, 1961., pp. 133-150
- [3] Robinson, H.E. "Thermal Conductivity Reference Standards." Proceedings of the Second Conference on Thermal Conductivity. Division of Applied Physics, National Research Council, Ottaws, Canada. October 10, 11, 12, 1962, pp. 311-322.

## APPENDIX A

### MATHEMATICAL ANALYSIS OF GEOMETRICAL FACTOR

It is important to note that this analysis is based on the change of heat flow in the annulus and through the boundaries of the annulus, so the equations and solution are based only on the annulus, and not on the cut-bar or the cylindrical guard; however, the boundary conditions are based on the temperature distribution of the cut-bar, the cylindrical guard, and the heater cooler system.

Mathematical investigation of the powder insulation annulus follows:

Figure A-1 shows a schematic of the cut-bar apparatus. The two meter bars are of equal length  $M$  and of the same thermal conductivity  $K_m$ .

$W$  - the overall length of the cut-bar

$M$  - the length of the meter-bar

$L$  - the length of the specimen bar

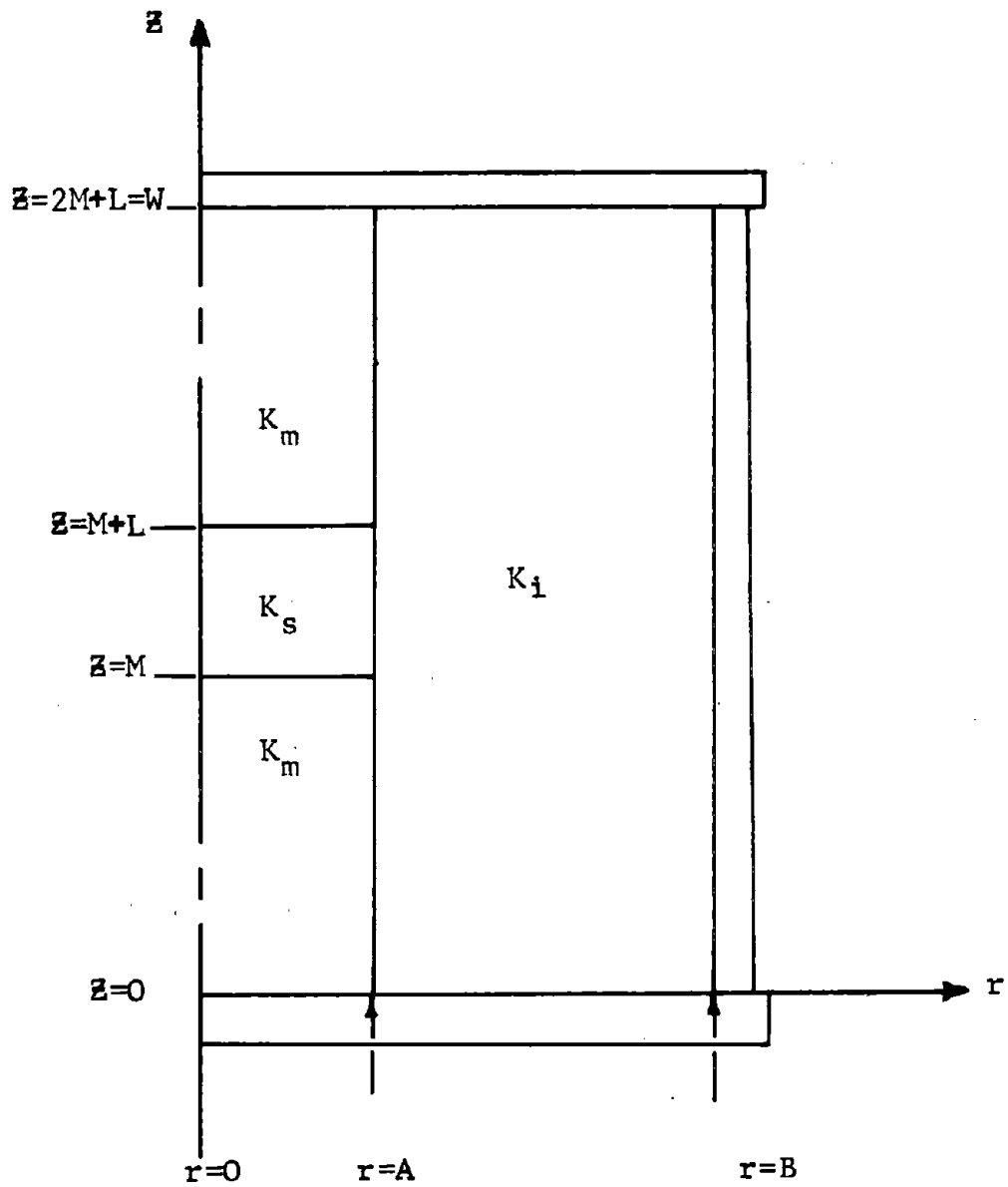
$A$  - the radius of the cut-bar, or the inner radius of the powder insulation annulus

$B$  - the outer radius of the powder insulation annulus or the inner radius of the cylindrical guard.

$K_m$  - the thermal conductivity of the meter-bar

FIGURE A-1

A SCHEMATIC OF THE CUT-BAR APPARATUS



$K_s$  - the thermal conductivity of the specimen bar

$K_i$  - the thermal conductivity of the powder insulation in the annulus

$V$  - the temperature variable

The boundary conditions of the powder insulation annulus are:

$$\begin{array}{lll}
 r = A & 0 \leq Z \leq W & V = G(Z) \\
 r = B & 0 \leq Z \leq W & V = H(Z) \\
 A = r = B & Z = 0 & V_1 = V = \text{Constant} \\
 & & G(0) = H(0) = V_1 \\
 A \leq r \leq B & Z = W & V = V_2 = \text{Constant} \\
 & & G(W) = H(W) = V_2 \quad (A-1)
 \end{array}$$

The above boundary conditions of the annulus may be reduced to dimensionless variables.

The dimensionless variables are:

$$\begin{array}{lll}
 u = \frac{Z}{W} & m = \frac{M}{W} & l = \frac{L}{W} \\
 \rho = \frac{r}{W} & a = \frac{A}{W} & b = \frac{B}{W} \\
 \theta = \frac{V - V_2}{V_1 - V_2} & \sigma_s = \frac{K_s}{K_m} & \sigma_i = \frac{K_i}{K_m} \quad (A-2)
 \end{array}$$

The dimensionless boundary conditions are:

$$\begin{aligned}
 \rho = a & \quad 0 \leq u \leq 1 & \theta = g(u) = \frac{G(Z) - V_2}{V_1 - V_2} \\
 \rho = b & \quad 0 \leq u \leq 1 & \theta = h(u) = \frac{H(Z) - V_2}{V_1 - V_2} \\
 a = \rho = b & \quad u = 0 & \theta = 1 \\
 a = \rho = b & \quad u = 1 & \theta = 0
 \end{aligned} \tag{A-3}$$

The governing differential equation of heat flow in the annulus is Laplace's equation in cylindrical coordinates:

$$\nabla^2 V = 0$$

Using dimensionless variables Laplace's equation is,

$$\frac{\partial^2 \theta}{\partial \rho^2} + \frac{1}{\rho} \frac{\partial \theta}{\partial \rho} + \frac{\partial^2 \theta}{\partial \omega^2} = 0 \tag{A-4}$$

Using separation of variables,

$$\theta = PE \tag{A-5}$$

Substituting equations (A-5) into (A-4):

$$\frac{P''}{P} + \frac{1}{\rho} \frac{P'}{P} + \frac{E''}{E} = 0$$

Therefore,

$$\frac{E''}{E} = -\alpha^2 \tag{A-6}$$

And,

$$P'' + \frac{1}{\rho} P' - \alpha^2 P = 0 \tag{A-7}$$

Solving equation (A-6),

$$E = C_1 \sin(\alpha u) + C_2 \cos(\alpha u) \quad (A-8)$$

Solving equation (A-7) the solution is in the form of Modified Bessel Functions:

$$P = C_3 I_0(\alpha \rho) + C_4 K_0(\alpha \rho) \quad (A-9)$$

Substituting equations (A-8) and (A-9) into (A-5):

$$\theta = \left[ C_3 I_0(\alpha \rho) + C_4 K_0(\alpha \rho) \right] \left[ C_1 \sin(\alpha u) + C_2 \cos(\alpha u) \right] \quad (A-10)$$

Applying the last boundary condition to (A-10):

$$a = \rho = b \quad u = 1 \quad \theta = 0$$

Then,

$$C_2 = 0 \quad \sin \alpha = 0 \quad \text{and} \quad \alpha = n\pi$$

Where,  $n = 0, 1, 2, \dots$  thus, equation (A-10) becomes:

$$\theta = C_0 + \sum_{n=1}^{\infty} \left[ C_n I_0(n\pi \rho) + D_n K_0(n\pi \rho) \right] \sin(n\pi u) \quad (A-11)$$

Using the other boundary conditions from equations (A-3):

$$a \leq \rho \leq b \quad u = 0 \quad \theta = 1$$

$$a = \rho = b \quad u = 1 \quad \theta = 0$$

Then,

$$C_0 = 1 - u$$



And,

$$\theta = 1 - u + \sum_{n=1}^{\infty} \frac{1}{n} \left[ C_n I_0(n\pi\rho) + D_n K_0(n\pi\rho) \right] \sin(n\pi u) \quad (A-12)$$

At the inner diameter of the annulus, using equation (A-12) the equation for the inner perimeter surface temperature is:

$$g(u) = (1-u) + \sum_{n=1}^{\infty} \frac{1}{n} \left[ C_n I_0(n\pi a) + D_n K_0(n\pi a) \right] \sin(n\pi u) \quad (A-13)$$

Correspondingly at the outer diameter of the annulus using equation (A-12) the equation of the outer perimeter surface is:

$$h(u) = (1-u) + \sum_{n=1}^{\infty} \frac{1}{n} \left[ C_n I_0(n\pi b) + D_n K_0(n\pi b) \right] \sin(n\pi u) \quad (A-14)$$

Letting,

$$a_n = C_n I_0(n\pi a) + D_n K_0(n\pi a) \quad (A-15)$$

$$b_n = C_n I_0(n\pi b) + D_n K_0(n\pi b) \quad (A-16)$$

Solving  $C_n$  and  $D_n$  from equations (A-15) and (A-16):

$$C_n = \frac{\begin{vmatrix} a_n & K_0(n\pi a) \\ b_n & K_0(n\pi b) \end{vmatrix}}{\begin{vmatrix} I_0(n\pi a) & K_0(n\pi a) \\ I_0(n\pi b) & K_0(n\pi b) \end{vmatrix}} \quad (A-17)$$

$$D_n = \frac{\begin{vmatrix} I_0(n\pi a) & a_n \\ I_0(n\pi b) & b_n \end{vmatrix}}{\begin{vmatrix} I_0(n\pi a) & K_0(n\pi a) \\ I_0(n\pi b) & K_0(n\pi b) \end{vmatrix}} \quad (A-18)$$

Substituting equations (A-15) into (A-13) and (A-16) into (A-14) and arranging so that:

$$u-1+g(u) = \sum_{n=1}^{\infty} a_n \sin(n\pi u) \quad (A-19)$$

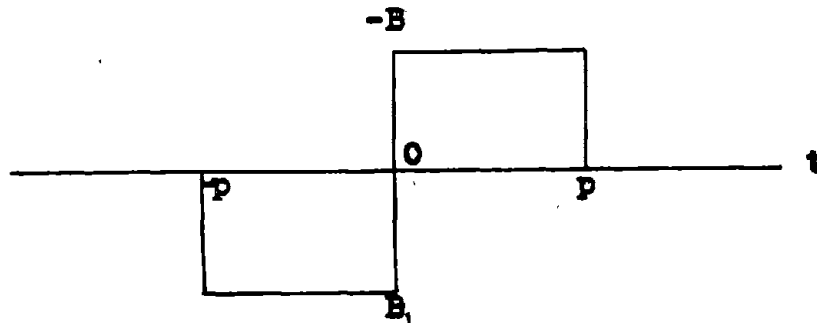
$$u-1+h(u) = \sum_{n=1}^{\infty} b_n \sin(n\pi u) \quad (A-20)$$

Solving for the Euler coefficients  $a_n$  and  $b_n$ , it is necessary to use Euler-Fourier formulas.<sup>1</sup>

The half-range sine expansion is based upon extending  $(u-1)+g(u)$  and  $(u-1)+h(u)$  over the interval  $u$  of  $(-1,0)$  by reflection in the origin.

---

1: Drawing



If  $BB_1$  is chosen as the vertical axis, the graph defines an odd function by the theorem only sine terms

If,

$p = 1$  and  $u = t$  (from footnote 1)

$a_n$  and  $b_n$  are:

$$a_n = 2 \int_0^1 [(u-1)+g(u)] \sin(n\pi u) du \quad (A-21)$$

$$b_n = 2 \int_0^1 [(u-1)+h(u)] \sin(n\pi u) du \quad (A-22)$$

Using the boundary conditions for a linear guard:

$$H(Z) = V_1 - (V_1 - V_2) \frac{Z}{W} \quad (A-23)$$

Substituting into equation (A-23) the dimensionless variables of the equation (A-2) and the boundary condition  $h(u)$  of equations (A-3):

$$h(u) = \frac{V_1 - (V_1 - V_2)u - V_2}{V_1 - V_2}$$

Thus,

$$h(u) = 1 - u \quad (A-24)$$

By substituting equation (A-24) into (A-22):

$$b_n = 0 \quad (A-25)$$

---

will appear in its expansion.

**Theorem:** If  $f(t)$  is an odd periodic function, then the coefficients in the Fourier series  $f(t)$  are given by the formulas:

$$A_n = 0 \quad B_n = \frac{2}{p} \int_0^p f(t) \sin\left(\frac{n\pi t}{p}\right) dt$$

The oddness depends upon the relation to the vertical axis of the coordinate system which can be arbitrarily chosen.

Differentiating equation (A-12):

$$\begin{aligned}\frac{d\theta}{d\rho} &= \sum_{n=1}^{\infty} n\pi \sin(n\pi u) \left[ C_n I_0'(n\pi\rho) + D_n K_0'(n\pi\rho) \right] \\ \frac{d\theta}{d\rho} &= \sum_{n=1}^{\infty} n\pi \sin(n\pi u) \left[ C_n I_1(n\pi\rho) - D_n K_1(n\pi\rho) \right] \quad (A-26)\end{aligned}$$

Let equation (A-26) define the surface of the annulus at the inner diameter A.

Substituting equations (A-17), (A-18), (A-25) into (A-26) the resulting equation for the inner diameter is:

$$\frac{\partial\theta}{\partial\rho} = \sum_{n=1}^{\infty} a_n n\pi \sin(n\pi u) \left[ \frac{K_0(n\pi b) I_1(n\pi a) + I_0(n\pi b) K_1(n\pi a)}{K_0(n\pi b) I_0(n\pi a) - I_0(n\pi b) K_0(n\pi a)} \right] \quad (A-27)$$

The radial heat flow at the inner surface of the annulus,  $r = A$ , through a cylindrical surface element of length  $dZ$  is:

$$dp = 2\pi A K_i \left( \frac{\partial v}{\partial r} \right)_{r=A} dZ \quad (A-28)$$

Using the dimensionless variables from the equations (A-2), equation (A-28) becomes:

$$dp = 2\pi a \sigma_i \left( \frac{\partial \theta}{\partial \rho} \right)_{\rho=a} du \quad (A-29)$$

The total dimensionless radial heat flow across the inner cylindrical surface of the annulus is found by integrating equation (A-29) for limits

between  $u = u_1$  to  $u = u_2$  which are defined in the analysis subsequently,

$$p(u)_1^2 = 2\pi a \sigma_i \int_{u_1}^{u_2} \frac{\partial \theta}{\partial r} \bigg|_{r=a} du \quad (\text{A-30})$$

Substituting equation (A-27) into (A-30) and integrating

$$p(u)_1^2 = \sum_{n=1}^{\infty} 2\pi a \sigma_i a_n \left[ \cos(n\pi u_1) - \cos(n\pi u_2) \right] \left[ \frac{K_0(n\pi b)I_1(n\pi a) + I_0(n\pi b)K_1(n\pi a)}{K_0(n\pi b)I_0(n\pi a) - I_0(n\pi b)K_0(n\pi a)} \right] \quad (\text{A-31})$$

It is necessary to define a temperature distribution along the inner surface of the annulus, which then defines  $a_n$ .

Referring to Figure A-1:  $V_1$  is the temperature at the matched end where  $Z = 0$ ;  $S_s$  is the constant longitudinal temperature gradient in the specimen bar; and  $S_m$  is the constant longitudinal temperature gradient in the meter-bar.

The boundary conditions of the cut-bar define the temperature distribution along the inner surface of the annulus. This temperature is constant around the perimeter which is equal distant from the ends.

$$\begin{aligned}
0 \leq Z \leq M & \quad V = T - S_m Z \\
M \leq Z \leq M+L & \quad V = T - S_m M - S_s (Z-M) \\
m + L \leq Z \leq W & \quad V = T - S_m M - S_s L - S_m (Z-M-L) = S_m (W-Z)
\end{aligned}
\tag{A-32}$$

Using the dimensionless variables of equations (A-2) the above boundary conditions (A-32) are re-defined for a dimensionless temperature distribution  $g(u)$ :

$$\begin{aligned}
0 \leq u \leq m & \quad \theta = 1 - \Psi_m u \\
m \leq u \leq m + l & \quad \theta = 1 - \Psi_m m - \Psi_s (u-m) \\
m + l \leq u \leq 1 & \quad \theta = \Psi_m (1-u)
\end{aligned}
\tag{A-33}$$

Where,

$$\Psi_m = \frac{S_m W}{T}, \quad \Psi_s = \frac{S_s W}{T}
\tag{A-34}$$

Using the above boundary conditions (A-33) and equation (A-21) the value for  $a_n$  can be defined as:

$$a_n = a_{n1} + a_{n2} + a_{n3}
\tag{A-35}$$

$$\begin{aligned}
a_{n1} &= 2 \int_0^m u (1 - \Psi_m) \sin(n \pi u) du \\
a_{n1} &= \frac{2(1 - \Psi_m)}{n^2 \pi^2} [\sin(n \pi m) - n \pi m \cos(n \pi m)]
\end{aligned}
\tag{A-36}$$

$$\begin{aligned}
a_{n2} &= 2 \int_m^{m+l} (-\Psi_m + \Psi_s) \sin(n\pi u) du \\
&+ 2 \int_m^{m+l} (1 - \Psi_s) u \sin(n\pi u) du \\
a_{n2} &= \frac{2m(\Psi_s - \Psi_m)}{n\pi} \left[ \cos(n\pi m) - \cos n\pi(m-l) \right] \\
&+ \frac{2(1 - \Psi_s)}{n^2 \pi^2} \left[ \sin(n\pi m + n\pi l) - n\pi(m+l) \cos(n\pi m + n\pi l) \right. \\
&\left. - \sin(n\pi m) + n\pi m \cos(n\pi m) \right] \quad (A-37)
\end{aligned}$$

$$\begin{aligned}
a_{n3} &= 2 \int_{m+l}^1 [\Psi_m - 1 + u(1 - \Psi_m)] \sin(n\pi u) du \\
a_{n3} &= \frac{2(\Psi_m - 1)}{n\pi} \left\{ \cos[n\pi(m+l)] - \cos(n\pi) \right\} \\
&+ \frac{2(1 - \Psi_m)}{n^2 \pi^2} \left[ -n\pi \cos(n\pi) - \sin(n\pi m + n\pi l) \right. \\
&\left. + n\pi(m+l) \cos(n\pi m + n\pi l) \right] \quad (A-38)
\end{aligned}$$

Substitute equations (A-36), (A-37), (A-38) into (A-35) and by arranging and reducing the Euler coefficients become:

$$a_n = \frac{4}{n^2 \pi^2} (\Psi_m - \Psi_s) \left[ \sin\left(\frac{n\pi l}{2}\right) \cos\left(\frac{n\pi}{2}\right) \right] \quad (A-39)$$

From equations (A-2) of dimensionless variables,

$$\sigma_s = \frac{K_s}{K_m} \quad (A-40)$$

Assuming that there is no heat loss or gain in the cut-bar, it is possible to help reduce the mathematical analysis so that the resulting solution can be solved by computer with only a minor loss in the accuracy of the resulting data.

Thus,

$$K_m S_m = K_s S_s$$

Or,

$$\frac{S_m}{S_s} = \frac{K_s}{K_m} \quad (A-41)$$

From equations (A-34), and (A-41) it can be shown that,

$$\frac{\Psi_s}{\Psi_m} = \frac{K_m}{K_s} \quad (A-42)$$

Let  $Q$  represent the total Longitudinal heat flow through the cut-bar with the stipulation that there be no heat gained or lost through the surface between the cut-bar and the annulus.

Thus,

$$Q = \pi A^2 K_m S_m = \pi A^2 K_s S_s \quad (A-43)$$

Defining heat flow  $Q$  in dimensionless parameters:

$$q = \frac{Q}{WTK_m} \quad (A-44)$$



Using equations (A-34), (A-43) and (A-44), we have,

$$q = \pi a^2 \psi_m \quad (\text{A-45})$$

Defining the net fraction of power lost or gained in the annulus between  $u = 0$  and  $u = u_2$  as  $\Omega$ . Heat loss in the cut-bar is the heat gained in the annulus; thus, the fractional power change  $\gamma$  in the cut-bar is,

$$\gamma = -\Omega = -\frac{p}{q} \quad (\text{A-46})$$

Substituting in values for  $p$ ,  $q$  into equation (A-46) by using equations (A-31), (A-39), (A-42), and (A-45):

$$\gamma = -K_1 \left( \frac{1}{K_m} - \frac{1}{K_s} \right) \frac{8}{\pi^2 a} \sum_{n=1}^{\infty} \left[ \frac{1 - \cos(n\pi u_2)}{n^2} \right] \left[ \frac{K_0(n\pi b)I_1(n\pi a) + I_0(n\pi b)K_1(n\pi a)}{K_0(n\pi b)I_0(n\pi a) - I_0(n\pi b)K_0(n\pi a)} \right] \sin\left(\frac{n\pi \rho}{2}\right) \cos\left(\frac{n\pi}{2}\right) \quad (\text{A-47})$$

Substituting the dimensionless variables of equation (A-2) into equation (A-47), equation (A-47) becomes:

$$\gamma = -K_1 \left( \frac{1}{K_s} - \frac{1}{K_s} \right) \frac{8W}{\pi^2 A} \sum_{n=1}^{\infty} \left[ \frac{1 - \cos\left(\frac{n\pi Z}{W}\right)}{n^2} \right] \left[ \frac{K_0\left(\frac{n\pi B}{W}\right)I_1\left(\frac{n\pi A}{W}\right) + I_0\left(\frac{n\pi B}{W}\right)K_1\left(\frac{n\pi A}{W}\right)}{K_0\left(\frac{n\pi B}{W}\right)I_0\left(\frac{n\pi A}{W}\right) - I_0\left(\frac{n\pi B}{W}\right)K_0\left(\frac{n\pi A}{W}\right)} \right] \sin\left(\frac{n\pi L}{2W}\right) \cos\left(\frac{n\pi}{2}\right) \quad (\text{A-48})$$

$\gamma$  is the per cent heat loss relative to the total heat flow in the cut-bar assuming that the total heat flow is the flow when there would be no loss or gain in the flow from or to the powder insulation annulus,

$\gamma$  is called the fractional power change.

Letting,

$$\gamma = F_k F_g \quad (A-49)$$

Where,

$$F_k = K_i \left( \frac{1}{K_m} - \frac{1}{K_s} \right) \quad (A-50)$$

$F_k$  is the thermal conductivity factor of the fractional power change;

And,

$$F_g = \frac{8W}{\pi^2 A} \sum_{n=1}^{\infty} \left[ \frac{1 - \cos\left(\frac{n\pi Z}{W}\right)}{n^2} \right] \left[ \frac{K_0\left(\frac{n\pi B}{W}\right) I_1\left(\frac{n\pi A}{W}\right) + I_0\left(\frac{n\pi B}{W}\right) K_1\left(\frac{n\pi A}{W}\right)}{K_0\left(\frac{n\pi B}{W}\right) I_0\left(\frac{n\pi A}{W}\right) - I_0\left(\frac{n\pi B}{W}\right) K_0\left(\frac{n\pi A}{W}\right)} \right] \sin\left(\frac{n\pi L}{2W}\right) \cos\left(\frac{n\pi}{2}\right) \quad (A-51)$$

It is necessary to simplify equation (A-51) for computer analysis since,

$$\cos\left(\frac{n\pi}{2}\right) = 0 \text{ when } n \text{ is odd}$$

Therefore,

$$(-1)^{\frac{n}{2}} = \cos\left(\frac{n\pi}{2}\right) \text{ when } n \text{ is even} \quad (\text{A-52})$$

$$\text{Letting, } m = \frac{n}{2} \quad (\text{A-53})$$

Substituting equations (A-53), (A-52) into equation (A-51), the index of equation (A-51) can be changed with no loss to the equation.

Therefore,

$$F_g = \frac{2W}{\pi^2 A} \sum_{m=1,2,\dots}^{\infty} (-1)^m \left[ \frac{1 - \cos\frac{2\pi Z_m}{W}}{m^2} \right] \left[ \frac{K_0\left(\frac{2m\pi B}{W}\right) I_1\left(\frac{2m\pi A}{W}\right) + I_0\left(\frac{2m\pi B}{W}\right) K_1\left(\frac{2m\pi A}{W}\right)}{K_0\left(\frac{2m\pi B}{W}\right) I_0\left(\frac{2m\pi A}{W}\right) - I_0\left(\frac{2m\pi B}{W}\right) K_0\left(\frac{2m\pi A}{W}\right)} \right] \sin\left(\frac{m\pi L}{W}\right) \quad (\text{A-54})$$

$F_g$  is the geometrical factor of the fractional change.

## APPENDIX B

### COMPUTER PROGRAM OF GEOMETRICAL FACTOR

A computer program was developed to calculate the large number of data points needed to plot the design charts. Also, this program was utilized in the error analysis of any particular apparatus. A particular range of design dimensions can be identified by the use of these charts. The exact error for a given set of dimensions can be found by using the program.

In Appendix A, the resulting solution is described in a mathematical equation (A-54) for the geometrical factor of the cut-bar apparatus. This equation is reproduced below:

$$F_g = \frac{2W}{\pi^2 A} \sum_{m=1,2,\dots}^{\infty} (-1)^m \left[ \frac{1 - \cos\left(\frac{2m\pi Z}{W}\right)}{m^2} \right]$$

$$\left[ \frac{K_0\left(\frac{2m\pi B}{W}\right) I_1\left(\frac{2m\pi A}{W}\right) + I_0\left(\frac{2m\pi B}{W}\right) K_1\left(\frac{2m\pi A}{W}\right)}{K_0\left(\frac{2m\pi B}{W}\right) I_0\left(\frac{2m\pi A}{W}\right) - I_0\left(\frac{2m\pi B}{W}\right) K_0\left(\frac{2m\pi A}{W}\right)} \right] \sin\left(\frac{m\pi L}{W}\right)$$

(B-1)

Two computer programming approaches are obvious. The first approach uses a large memory bank where all of the Modified Bessel Function of the first and second kind, and of the first and second order, are

stored. Using this method, it is necessary to use approximation techniques to find the Modified Bessel Functions of fractional arguments. This method can be used only in a data reduction center having the necessary facilities. The second approach is to generate the Modified Bessel Function in a program when needed.

The second approach was used in this thesis because the IBM 1620 Computer which was available was limited in size and speed, and the computer program using the Fortran language was efficient. The program can function in the Fortran II, Fortran IV, or Forgo language, and with a small change it can function in PDQ language.

Inputs into the following programs are: W, A, B, CL, TEST, JA, MM, LP.

- W - length of the annulus.
- A - the diameter of the specimen bar and meter-bar, or the inner diameter of the annulus.
- B - the outer diameter of the annulus or the inner diameter of the cylindrical guard.
- CL- the longitudinal length of the specimen bar. It is represented by L in the equation (B-1).
- TEST- the accuracy of the resulting output  $F_g$ . TEST stops the program or truncates the series when it has converged so the  $F_g$  is varying within the range of the TEST input.

- JA - the number of points for which  $F_g$  output is formed along one-half of the bar. It is the number of Z points into which one-half of the bar is divided.
- MM - the limiting number of terms in the series. It represents the maximum number of terms at which the series or program will be truncated. At some points, the series will converge only at a very large number of terms.
- LP - the frequency of the test for convergence of the series. It must be an odd number and it is based on the  $\frac{2W}{L}$ . With familiarity in using the program, an engineer's intuitiveness can find a reasonable LP.

Figure B-1 illustrates the flow-chart for the computer program. Three computer programs were developed based on this flow-chart and the available facilities. The computer program illustrated in Figure B-2 was developed for use on an IBM-1620 computer. Using this program as a source deck, an objective deck can be compiled in Fortran II and PDQ. This program can be used directly in Fargo language. Figure B-3 illustrates a computer program which can be used on a time-sharing-computer system, using Fortran IV language, and this program can be modified with the addition of the program statement lines illustrated in Figure B-4. This modification expands the program so that a large amount of data can be handled.

FIGURE B-1

COMPUTER PROGRAM FLOW-CHART

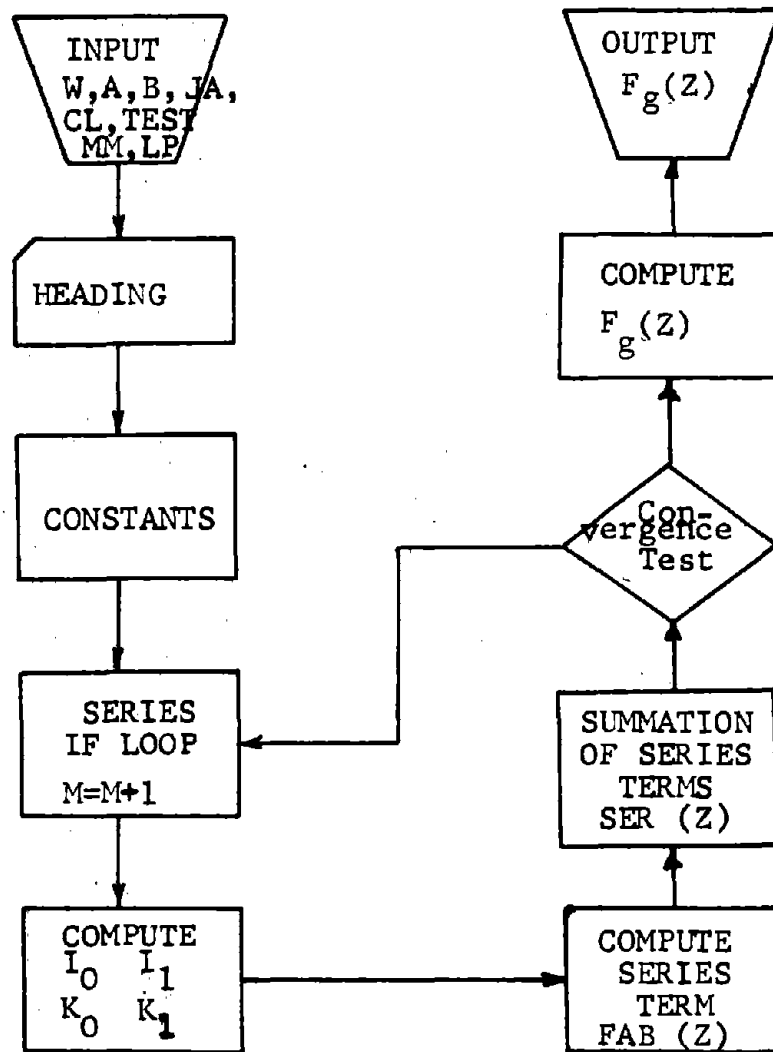


FIGURE B-2

COMPUTER PROGRAM FOR IBM-1620 COMPUTER

```
DIMENSION FAB(20),FB(20),Z(20),FG(20),SER(20),
BST(20),KL(20)

PI=3.1415927

GAM=.57721566

PUNCH 910

10 READ 905,W,A,B,CL,TEST,JA,MM,LP

PUNCH 920,JA

PUNCH 930

PUNCH 935,W,A,B,CL,TEST,JA,MM,LP

SIGN = 1.

EP = 1.

DOG = 1.

ENT = EXPF((-4.*(B-A)*PI)/W)

H = (2.0*W)/(PI*PI*A)

CAT = JA

DO 20 N= 1,JA

ZA = N

Z (N) = ZA*W/(2.*CAT)

SER(N)=0.0

BST(N)=9999.

KL(N)=0

20 FAB(N)=1.0

M=0
```



```

30  M=M+1

    DOG=DOG*ENT
    V=M
    XV=2.*V*PI/W
    RRI=V*PI/CAT
    SIGN= -SIGN
    Y=SINF(V*PI*CL/W)*SIGN/(V*V)
    X=A*XV
    CKS=X
    KK=0

40  NORD=0
500 BK=0.0
    FN=NORD
    IF(X-FN-6.)501,700,700
501 XA=X/2.
    XB=XA*XA
    N=0
503 AN=N
    T=1.
    S= -1.
510 IF(AN)9999,520,512
512 T=T*XA/AN
    AN=AN-1.
    GO TO 510

```

```

520  BIN=T
      DO 530 K=1,9999
      DEN=K*(K+N)
      T=T*XB/DEN
      IF((BIN+T)-BIN)525,550,525
525  BIN=BIN+T
530  CONTINUE
550  IF(N-1)575,630,555
555  IF(X-FN-3.)1111,1111,700
565  N=1
      BIO=BIN
      BKO=BK
      GO TO 503
575  BK= -(GAM+LOGF(XA))*BIN
      T=XB
      S=1.
      XI=1.
      DO 610 K=2,9999
      AK=K
      IF((BK+T*XI)-BK)600,620,600
600  BK=BK+T*XI
      T=T*XB/(AK*AK)
      XI=XI+1./AK
610  CONTINUE
620  IF(NORD)9999,555,565

```

```

630  BK=(1./X-BIN*BKO)/BIO
      IF(NORD-1)9999,555,9999
700  C=4*NORD*NORD
      D=8.*X
      CON2=1./SQRTF(2.*PI*X)
      CON3=SQRTF(PI/(2.*X))
      AN=NORD
      PHI=X-(2.*AN+1.)/4.*PI
      K=X+1.+SQRTF(X*X+AN*AN)
      T=(C-1.)/D
      S=1.
      U=1.
      PN=1.
      QN=T
      BK=1.+T
      BI=1.-T
      DO 735 I=2,K
      AI=I
      T=(C-(2.*AI-1.))**2/D*T/AI
      BK=BK+T
      BI=BI+T*S
      IF((BI+T)-BI)730,738,730
730  S= -S
735  CONTINUE

```

```

738  IF(CKS-7.)741,755,755
741  BK=EXPF(-X)*CON3*BK
      IF(X-FN-6.)1111,750,750
750  BIN=EXPF(X)*CON2*BI
      GO TO 1111
755  BK=CON3*BK
760  BIN=CON2*BI
      EP=DOG
1111  NORD=FN
      IF(NORD)9999,810,830
810  IF(KK)9999,820,840
820  GA=BIN
      GB=BK
      NORD=1
      GO TO 500
830  GC=BIN
      GD=BK
      X=XV*B
      KK=1
      GO TO 40
840  GE=BIN
      GF=BK*EP
      R=(GF*GC+GE*GD)/(GF*GA-GE*GB)
      FA=Y*R

```

```

        LPF=0
        DO 860 N=1,JA
            IF(KL(N)-3)845,850,858
845     LPF=1
850     ZA=N
        FB(N)=1.0-COSF(RRI*ZA)
        FAB(N)=FA*FB(N)
        SER(N)=SER(N)+FAB(N)
        IF(M/LP*LP-M)860,852,860
852     IF(TEST-ABS(BST(N)-SER(N)))854,856,856
854     KL(N)=0
        BST(N)=SER(N)
        GO TO 860
856     BST(N)=SER(N)
858     KL(N)=KL(N)+1
860     CONTINUE
        IF(LPF-1)890,888,9999
888     IF(M-MM)30,890,890
890     PUNCH 960,M
        DO 900 J=1,JA
            FG(J)=H*SER(J)
900     PUNCH 940,J,Z (J),KL(J),SER(J),FG(J)
        GO TO 10
9999    PUNCH 9998
        GO TO 10
905     FORMAT (5F10.5,3I5)

```

```
910  FORMAT (///12X,46HRESULTS OF POWER LOSS OVER  
      LENGTH OF METER-BAR//)  
  
920  FORMAT (///12X,15HFG VERSUS Z FOR,I3,23H  
      POINTS FROM Z=0 TO END//)  
  
930  FORMAT (6X,1HW,9X,1HA,9X,1HB,9X,1HL,8X,4HTEST,  
      5X,1HP,3X,1HM,4X,1HF)  
  
935  FORMAT (5F10.5,3I5//)  
  
940  FORMAT (I10,F14.5,I8,3X,2F10.7)  
  
960  FORMAT (//7X,5HPOINT,8X,1HZ,9X,2HKL,7X,3HSER,  
      8X,2HFG,5X,2HM=,I3)  
  
9998 FORMAT (//25X,5HERROR//)  
  
      END
```

FIGURE B-3

COMPUTER PROGRAM FOR TIME-SHARING COMPUTER

```
10  DIMENSION FAB(30),FB(30),Z(30),FG(30),SER(30),  
    BST(30),KL(30)  
20  PI=3.1415927  
30  GAM=.57721566  
40  PRINT 910  
50  10 INPUT,W,A,B,CL,TEST,JA,MM,LP  
60  PRINT 920,JA  
70  PRINT 930  
80  PRINT 935,W,A,B,CL,TEST,JA,MM,LP  
85  SIGN=1.  
90  EP=1.  
100 DOG=1.  
110 ENT=EXP((-4.*(B-A)*PI)/W)  
120 H=(2.0*W)/(PI*PI*A)  
130 CAT=JA  
140 DO 20 N=1,JA  
150  ZA=N  
160  Z(N)=ZA*W/(2.*CAT)  
170  SER(N)=0.0  
180  BST(N)=9999.  
190  KL(N)=0  
200  20 FAB(N)=1.0
```

```

210  M=0
220  30 M=M+1
230  DOG=DOG*ENT
240  V=M
245  XV=2.*V*PI/W
248  SIGN= -SIGN
250  Y=SINF(V*PI*CL/W)*SIGN/(V*V)
260  RRI=V*PI/CAT
280  X=A*XV
290  CKS=X
300  KK=0
330  40 NORD=0
340  500 BK=0.0
350  FN=NORD
360  IF(X-FN-6.)501,700,700
370  501 XA=X/2.
380  XB=XA*XA
390  N=0
400  503 AN=N
405  T=1.
410  S= -1.
415  510 IF(AN)9999,520,512
420  512 T=T*XA/AN
425  AN=AN-1.
430  GO TO 510

```



```

435 520 BIN=T
440 DO 530 K=1,9999
445 DEN=K*(K+N)
450 T=T*XB/DEN
455 IF((BIN+T)-BIN)525,530,525
460 525 BIN=BIN+T
465 530 CONTINUE
470 550 IF(N-1)575,630,555
475 555 IF(X-FN-3.)1111,1111,700
480 565 N=1
485 BIO=BIN
490 BKO=BK
495 GO TO 503
500 575 BK= -(GAM+LOGF(XA))*BIN
505 T=XB
510 S=1.
515 XI=1.
520 DO 610 K=2,9999
525 AK=K
530 IF((BK+T*XI)-BK)600,620,600
535 600 BK=BK+T*XI
540 T=T*XB/(AK*AK)
545 XI=XI+1./AK
550 610 CONTINUE
555 620 IF(NORD)9999,555,565

```

```

560 630 BK=(1./X-BIN*BKO)/BIO
565 IF(NORD-1)9999,555,9999
570 700 C=4*NORD*NORD
575 D=8.*X
580 CON2=1./SQRTF(2.*PI*X)
585 CON3=SQRTF(PI/(2.*X))
590 AN=NORD
600 PHI=X-(2.*AN+1.)/4.*PI
602 K=X+1.+SQRTF(X*X+AN*AN)
604 T=(C-1.)/D
606 S=1.
608 U=1.
610 PN=1.
612 QN=T
614 BK=1.+T
616 BI=1.-T
618 DO 735 I=2,K
620 AI=I
622 T=(C-(2.*AI-1.))**2)/D*T/AI
624 BK=BK+T
626 BI=BI+T*S
628 IF((BI+T)-BI)730,738,730
630 730 S= -S
632 735 CONTINUE

```

```

634 738 IF(CKS-7.)741,755,755
636 741 BK=EXPF(-X)*CON3*BK
638 IF(X-FN-6.)1111,750,750
640 750 BIN=EXPF(X)*CON2*BI
642 GO TO 1111
644 755 BK=CON3*BK
646 760 BIN=CON2*BI
648 EP=DOG
650 1111 NORD=FN
652 IF(NORD)9999,810,830
654 810 IF(KK)9999,820,840
656 820 GA=BIN
658 GB=BK
660 NORD=1
662 GO TO 500
664 830 GC=BIN
666 GD=BK
668 X=XV*B
670 KK=1
672 GO TO 40
674 840 GE=BIN
676 GF=BK*EP
678 R=(GF*GC+GE*GD)/(GF*GA-GE*GB)
680 FA=Y*R

```

```

682   LPF=0
684   DO 860 N=1,JA
686   IF(KL(N)-3)845,850,858
688   845 LPF=1
690   850 ZA=N
692   FB(N)=1.0-COSF(RRI*ZA)
694   FAB(N)=FA*FB(N)
696   SER(N)=SER(N)+FAB(N)
698   IF(M/LP*LP-M)860,852,860
700   852 IF(TEST-ABS(BST(N)-SER(N)))854,856,856
702   854 KL(N)=0
704   BST(N)=SER(N)
706   GO TO 860
708   856 BST(N)=SER(N)
710   858 KL(N)=KL(N)+1
712   860 CONTINUE
714   IF(LPF-1)890,888,9999
716   888 IF(M-MM)30,890,890
718   890 PRINT 960,M
720   DO 900 J=1,JA
722   FG(J)=H*SER(J)
724   900 PRINT 940,J,Z (J),KL(J),SER(J),FG(J)
726   GO TO 10
728   9999 PRINT 9998

```

730 GO TO 10

732 910 FORMAT (//12X,46HRESULTS OF POWER LOSS  
OVER LENGTH OF METER-BAR//)

734 920 FORMAT (///12X,15HFG VERSUS Z FOR, I3,  
23H POINTS FROM Z=0 TO END//)

736 930 FORMAT (6X,1HW,9X,1HA,9X,1HB,9X,1HL,8X,  
4HTEST,5X,1HP,3X,1HM,4X,1HF)

738 935 FORMAT (5F10.5,3I5//)

740 940 FORMAT (I10,F14.5,I8,3X,2F10.7)

742 960 FORMAT (//7X,5HPOINT,8X,1HZ,9X,2HKL,7X,  
3HSER,8X,2HFG,5X,2HM=,I3)

744 9998 FORMAT (//25X,5HERROR//)

746 END

FIGURE B-4

COMPUTER PROGRAM FOR TIME-SHARING COMPUTER

50 10 READ,W,A,B,CL,TEST,JA,MM,LP  
746 \$DATA

TECHNICAL REPORTS DISTRIBUTION LIST, CONTRACT NONr 2249(12)

Office of Naval Research (5)  
Department of the Navy  
Washington, D. C. 20360  
ATTN: Code 429

Naval Ship Engineering Center (5)  
Department of the Navy  
Washington, D. C. 20360  
ATTN: Library (2), Code 6645 (3)

Naval Air Systems Command (5)  
Department of the Navy  
Washington, D. C. 20360  
ATTN: Library

Director  
Naval Research Laboratory (7)  
Washington 25, D. C.  
ATTN: Technical Information Div.

Marine Engineering Laboratory  
Annapolis, Maryland (2)

U. S. Naval Postgraduate School (2)  
Monterey, California  
ATTN: Library

Office of the Asst. (1)  
Chief of Staff, G-4  
Research and Development Div.  
Department of the Army  
Washington, D. C. 20360

Defense Documentation Center (20)  
Cameron Station  
Alexandria, Virginia

U. S. Army (1)  
Ordnance Missile Command  
Army Ballistic Missile Agency  
Redstone Arsenal, Alabama  
ATTN: ORDAB-RRT

U. S. Atomic Energy Commission (2)  
Technical Information Service  
P. O. Box 62  
Oak Ridge, Tennessee

Director (1)  
Engineering Res. and Dev. Lab  
Fort Belvoir, Virginia  
ATTN: Head, Nuclear Power Branch

U. S. Coast Guard Hq. (1)  
Testing and Development Div.  
1300 "E" Street  
Washington, D. C.

National Aeronautics and (1)  
Space Administration  
Ames Research Center  
Moffett Field, California  
ATTN: Library

National Aeronautics and (1)  
Space Administration  
Langley Research Center  
Langley Field  
Hampton, Virginia  
ATTN: Library

National Aeronautics and (2)  
Space Administration  
Lewis Research Center  
21000 Brookpark Road  
Cleveland 35, Ohio  
ATTN: Library

The Babcock and Wilcox Co. (1)  
Research and Dev. Center  
P. O. Box 835  
Alliance, Ohio

Battelle Memorial Institute (1)  
505 King Avenue  
Columbus 1, Ohio

Brookhaven National Laboratory (1)  
Technical Information Division  
Upton, Long Island, New York  
ATTN: Research Library

Electric Boat Company (2)  
Groton, Connecticut  
ATTN: Mr. E. S. Dennison

TECHNICAL REPORTS DISTRIBUTION LIST, CONTRACT NOnr 2249(12) (Cont'd)

Carrier Corporation (1)  
300 South Geddes Street  
Syracuse 1, New York  
ATTN: Engineering Library

General Motors Corp. (2)  
Allison Division  
Indianapolis 6, Indiana  
ATTN: Mr. R. M. Hazen,  
Dir. of Engrg.

General Motors Corp (2)  
Research Laboratories  
12 Mile and Mound Roads  
Warren, Michigan

California Inst. of Technology (1)  
Mechanical Engineering Dept.  
1201 East California Street  
Pasadena 4, California  
ATTN: Mechanical Engrg. Library

University of California (1)  
College of Engineering  
Berkeley 4, California

University of California at (1)  
Los Angeles  
Engineering Department  
Los Angeles 24, California

The Catholic University of America (1)  
Department of Mechanical Engineering  
Washington 17, D. C.

Columbia University (1)  
Heat Transfer Research Facility  
P. O. Box 245, Station J  
New York 27, New York

Cornell University (1)  
College of Engineering  
Dept. of Heat Power Engrg.  
Ithaca, New York

University of Houston (1)  
Mechanical Engineering Dept.  
Houston, Texas

Illinois Inst. of Technology (1)  
Dept. of Mechanical Engrg.  
Technology Center  
Chicago 16, Illinois  
ATTN: Heat Transfer Lab

University of Illinois (1)  
Mechanical Engineering Department  
Urbana, Illinois

Massachusetts Inst. of Tech. (1)  
Cambridge 39, Massachusetts  
ATTN: Prof. William H. McAdams

University of Michigan (1)  
228 W. Engineering Bldg.  
Ann Arbor, Michigan

University of Minnesota (1)  
Mechanical Engineering Dept.  
Minneapolis, Minnesota  
ATTN: Dr. E. R. G. Eckert

General Electric Company (2)  
Small Aircraft Engine Dept.  
1000 Western Ave.  
West Lynn 3, Massachusetts  
ATTN: Marine Industrial Market  
Development  
(Internal Distribution by Company)

General Electric Company (2)  
Cincinnati 15, Ohio  
ATTN: Mr. M. E. Lapides,  
Aircraft  
Nuclear Propulsion Department

General Electric Company (2)  
General Engineering Lab  
Schenectady 5, New York  
(Internal Distribution by Company)

Lockheed Aircraft Corp. (2)  
Missile Systems Division  
Aerodynamics Dept.  
Sunnyvale, California  
ATTN: Mr. G. A. Etemad



TECHNICAL REPORTS DISTRIBUTION LIST, CONTRACT NO nr 2249(12) (Cont'd)

Ford Motor Company (1)  
Dearborne, Michigan  
ATTN: Mrs. Rachel MacDonald  
Eng. Staff Library

The Franklin Institute (1)  
Laboratories for Research and Dev.  
Philadelphia 3, Pa.  
ATTN: Mr. F. L. Jackson

General Dynamics Corp. (2)  
General Atomic Division  
P. O. Box 608  
San Diego 12, California

Westinghouse Electric Corp. (2)  
Lester Branch P. O.  
Philadelphia 13, Pennsylvania  
ATTN: Mr. F. K. Fischer, Mgr.  
Dev. Engrg.

Modine Manufacturing Co. (2)  
1500 DeKoven Avenue  
Racine, Wisconsin  
ATTN: Mr. C. T. Perkins, Pres.

Morgantown Research Center (1)  
Bureau of Mines  
Morgantown, West Virginia  
ATTN: Mr. J. McGee

North American Aviation, Inc. (1)  
International Airport  
Los Angeles 45, California

United Aircraft Corp. (2)  
400 Main Street  
East Hartford 8, Conn.  
ATTN: Mr. Robert C. Sale  
Chief Librarian

The Trane Company (2)  
2nd and Cameron Avenue  
La Crosse, Wisconsin

Solar Aircraft Company (1)  
San Diego 12, California  
ATTN: Mr. P. A. Pitt,  
Chief Engineer

Worthington Corp. (2)  
Harrison Division  
Harrison, New Jersey  
ATTN: Mr. Normal L. Myerson,  
Director of Research

Young Radiator Company (2)  
703 S. Marquette Street  
Racine, Wisconsin  
ATTN: Mr. H. P. Brinen,  
Res. Engineer



Unclassified

Security Classification

## DOCUMENT CONTROL DATA - R&amp;D

(Security classification of title, body of abstract and indexing annotation must be entered when the overall report is classified)

|  |  |  |                      |
|--|--|--|----------------------|
| 1. ORIGINATING ACTIVITY (Corporate author)<br>The Catholic University of America<br>Department of Mechanical Engineering<br>Washington, D. C. 20017  |  | 2a. REPORT SECURITY CLASSIFICATION<br>Unclassified   |                      |
|  |  | 2b. GROUP  |                      |
| 3. REPORT TITLE<br>An Analysis and Design of a Linear Guarded Cut-Bar Apparatus for Thermal Conductivity Measurements  |  |  |                      |
| 4. DESCRIPTIVE NOTES (Type of report and inclusive dates)<br>Technical Report  |  |  |                      |
| 5. AUTHOR(S) (Last name, first name, initial)<br>David A. Didion   |  |  |                      |
| 6. REPORT DATE<br>31 Jan 1968  |  | 7a. TOTAL NO. OF PAGES<br>71   | 7b. NO. OF REFS<br>3 |
| 8a. CONTRACT OR GRANT NO.<br>NONr 2249(12)   |  | 9a. ORIGINATOR'S REPORT NUMBER(S)<br>Technical Report No. 2  |                      |
| b. PROJECT NO.   |  | 9b. OTHER REPORT NO(S) (Any other numbers that may be assigned this report)  |                      |
| c.   |  |  |                      |
| d.   |  |  |                      |
| 10. AVAILABILITY/LIMITATION NOTICES<br>Qualified Requesters may obtain copies of this report from D.D.C.   |  |  |                      |
| 11. SUPPLEMENTARY NOTES  |  | 12. SPONSORING MILITARY ACTIVITY<br>Office of Naval Research<br>Power Branch (Code 429)<br>Washington, D. C. 20390 |                      |
| 13. ABSTRACT<br>→ A quantitative analysis of the Cut-Bar method of measuring the thermal conductivity of solids is performed. The mathematical model, which corrects for the difference in heat flux in the specimen and reference standard, is that of the two dimensional steady heat conduction equation applied to an annulus of insulation. The solution is presented in detail and found to be comprised of two physically distinct parts, a conductivity factor and a geometrical factor. A number of charts and graphs are presented for clarification as to the nature and magnitude the relative sizes of the various components will have on the accuracy over different conductivity ranges. The complexity of the geometrical factor required a digital computer programs which are included. Reference is made to a similar study, performed by researchers at the National Bureau of Standards. It is found that the differences in the guard temperature distribution results in a substantial change in the geometrical factor. ( ) |  |  |                      |

Unclassified

## Security Classification

|   |        |    |        |    |        |    |
|---|--------|----|--------|----|--------|----|
| 14. KEY WORDS   | LINK A |    | LINK B |    | LINK C |    |
|   | ROLE   | WT | ROLE   | WT | ROLE   | WT |
| Thermal Conductivity<br>Measurements<br>Heat Conduction |        |    |        |    |        |    |

## INSTRUCTIONS

1. **ORIGINATING ACTIVITY:** Enter the name and address of the contractor, subcontractor, grantee, Department of Defense activity or other organization (*corporate author*) issuing the report.

2a. **REPORT SECURITY CLASSIFICATION:** Enter the overall security classification of the report. Indicate whether "Restricted Data" is included. Marking is to be in accordance with appropriate security regulations.

2b. **GROUP:** Automatic downgrading is specified in DoD Directive 5200.10 and Armed Forces Industrial Manual. Enter the group number. Also, when applicable, show that optional markings have been used for Group 3 and Group 4 as authorized.

3. **REPORT TITLE:** Enter the complete report title in all capital letters. Titles in all cases should be unclassified. If a meaningful title cannot be selected without classification, show title classification in all capitals in parenthesis immediately following the title.

4. **DESCRIPTIVE NOTES:** If appropriate, enter the type of report, e.g., interim, progress, summary, annual, or final. Give the inclusive dates when a specific reporting period is covered.

5. **AUTHOR(S):** Enter the name(s) of author(s) as shown on or in the report. Enter last name, first name, middle initial. If military, show rank and branch of service. The name of the principal author is an absolute minimum requirement.

6. **REPORT DATE:** Enter the date of the report as day, month, year; or month, year. If more than one date appears on the report, use date of publication.

7a. **TOTAL NUMBER OF PAGES:** The total page count should follow normal pagination procedures, i.e., enter the number of pages containing information.

7b. **NUMBER OF REFERENCES:** Enter the total number of references cited in the report.

8a. **CONTRACT OR GRANT NUMBER:** If appropriate, enter the applicable number of the contract or grant under which the report was written.

8b, 8c, & 8d. **PROJECT NUMBER:** Enter the appropriate military department identification, such as project number, subproject number, system numbers, task number, etc.

9a. **ORIGINATOR'S REPORT NUMBER(S):** Enter the official report number by which the document will be identified and controlled by the originating activity. This number must be unique to this report.

9b. **OTHER REPORT NUMBER(S):** If the report has been assigned any other report numbers (*either by the originator or by the sponsor*), also enter this number(s).

10. **AVAILABILITY/LIMITATION NOTICES:** Enter any limitations on further dissemination of the report, other than those

imposed by security classification, using standard statements such as:

- (1) "Qualified requesters may obtain copies of this report from DDC."
- (2) "Foreign announcement and dissemination of this report by DDC is not authorized."
- (3) "U. S. Government agencies may obtain copies of this report directly from DDC. Other qualified DDC users shall request through \_\_\_\_\_."
- (4) "U. S. military agencies may obtain copies of this report directly from DDC. Other qualified users shall request through \_\_\_\_\_."
- (5) "All distribution of this report is controlled. Qualified DDC users shall request through \_\_\_\_\_."

If the report has been furnished to the Office of Technical Services, Department of Commerce, for sale to the public, indicate this fact and enter the price, if known.

11. **SUPPLEMENTARY NOTES:** Use for additional explanatory notes.

12. **SPONSORING MILITARY ACTIVITY:** Enter the name of the departmental project office or laboratory sponsoring (*paying for*) the research and development. Include address.

13. **ABSTRACT:** Enter an abstract giving a brief and factual summary of the document indicative of the report, even though it may also appear elsewhere in the body of the technical report. If additional space is required, a continuation sheet shall be attached.

It is highly desirable that the abstract of classified reports be unclassified. Each paragraph of the abstract shall end with an indication of the military security classification of the information in the paragraph, represented as (TS), (S), (C), or (U).

There is no limitation on the length of the abstract. However, the suggested length is from 150 to 225 words.

14. **KEY WORDS:** Key words are technically meaningful terms or short phrases that characterize a report and may be used as index entries for cataloging the report. Key words must be selected so that no security classification is required. Identifiers, such as equipment model designation, trade name, military project code name, geographic location, may be used as key words but will be followed by an indication of technical context. The assignment of links, roles, and weights is optional.